IX
Lattice dynamics of crystals

In the previous chapter we have laid down the basic concepts of the quantum mechanical theory of electrons and nuclei in mutual interaction. According to the adiabatic principle, the system of light particles (the electrons) is preliminarly studied with the heavy particles (the nuclei) fixed in a given spatial configuration; the total ground-state energy of the electronic system, thought of as a function of the nuclear coordinates, becomes then the potential energy for the nuclear motion. We are interested here in small displacements around the equilibrium configuration of the ground adiabatic energy surface (supposed to be non-degenerate). Within the harmonic approximation, we describe the dispersion curves for normal mode propagation in crystals, and introduce the concept of *phonons*, as travelling quanta of vibrational energy. In the study of the lattice vibrations of ionic or partially ionic crystals (polar crystals), essentially new features appear in the long-wavelength limit; in polar crystals, the coupling of optical vibrational branches with the electromagnetic field leads to the concept of mixed phonon–photon quasiparticles, known as *polaritons*.

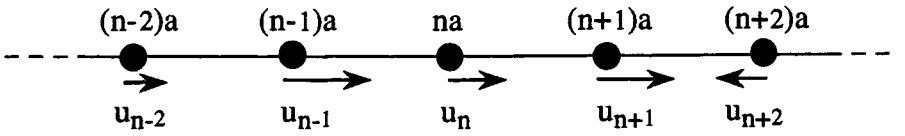

Fig. 1 Longitudinal displacements in a one-dimensional monatomic lattice. The equilibrium positions $t_n = na$ are indicated by circles; the displacements u_n at a given instant are indicated by arrows.

1 Dynamics of monatomic one-dimensional lattices

To describe the lattice vibrations of crystals, we consider first linear chains of equal atoms (present section), then linear chains with a basis of different atoms (Section 2), and finally general three-dimensional structures (Section 3). This sequence of increasing sophistication is adopted because some physical concepts are better illustrated in one-dimensional situations, where notations and technicalities can be kept at the essential.

So, we begin by considering a one-dimensional chain, of lattice constant a, formed by a (large) number N of atoms of mass M. We indicate by u_n the (longitudinal) displacement of the n-th atom from the equilibrium position $t_n = na$, at a particular time (see Fig. 1). We denote by $E_0(\{u_n\})$ the total ground-state energy of the crystal Hamiltonian, with the *nuclei fixed in the positions* $R_n = na + u_n$; the energy $E_0(\{u_n\})$ is also called *static lattice energy*. The ground state of the crystal is supposed to be non-degenerate for all configurations $\{u_n\}$ of interest.

In agreement with the general adiabatic principles of Section VIII-2, the total ground-state energy $E_0(\{u_n\})$ of the interacting electronic-nuclear system, with the nuclei fixed in the configuration u_n, becomes the "potential energy" for the nuclear motion. It is also assumed that, the forces $F_i = -\partial E_0(\{u_n\})/\partial u_i$ acting on the nuclei depend on the instantaneous nuclear positions $\{u_n\}$; retardation effects due to the finite propagation velocity of light are neglected at this stage and must be properly included, whenever necessary (see Section 7).

In the study of small oscillations, it is convenient to expand the total ground-state energy $E_0(\{u_n\})$ in increasing powers of the displacements u_n; we have the Taylor expansion

$$E_0(\{u_n\}) = E_0(0) + \frac{1}{2}\sum_{n\,n'}\left(\frac{\partial^2 E_0}{\partial u_n \partial u_{n'}}\right)_0 u_n u_{n'} + \frac{1}{3!}\sum_{n\,n'\,n''}\left(\frac{\partial^3 E_0}{\partial u_n \partial u_{n'}\,\partial u_{n''}}\right)_0 u_n u_{n'} u_{n''} + \dots \tag{1}$$

(derivatives evaluated at the equilibrium configuration carry the subscript 0). In the expansion (1), the linear terms in the displacements are not present since $\partial E_0/\partial u_n = 0$ at the equilibrium configuration. The total ground-state energy $E_0(0)$ at the equilib-

rium configuration is important in the discussion of the cohesive energy, but irrelevant in the discussion of lattice vibrations. The truncation to quadratic terms in the expression (1) is called "harmonic approximation"; in general the anharmonic terms (cubic, quartic terms and so on) are taken into account only after the harmonic approximation has been carried out.

In the harmonic approximation, which is appropriate for sufficiently small displacements, the total crystal energy (1) becomes

$$E_0^{(\mathrm{harm})}(\{u_n\}) = E_0(0) + \frac{1}{2}\sum_{n\,n'} D_{nn'}u_n u_{n'} \ , \tag{2}$$

where

$$D_{nn'} = \left(\frac{\partial^2 E_0}{\partial u_n \partial u_{n'}}\right)_0 \tag{3}$$

denote the second derivatives of the static lattice energy $E_0(\{u_n\})$ evaluated at the equilibrium configuration. The quantities $D_{nn'}$ are called *force constants*, and the matrix D formed with the force constants $D_{nn'}$ is called *force-constant matrix*. The force constants $D_{nn'}$ represent the proportionality coefficients connecting the forces acting on the nuclei with the displacements suffered by the nuclei; in the harmonic approximation, in fact we have

$$F_n = -\frac{\partial E_0^{(\mathrm{harm})}}{\partial u_n} = -\sum_{n'} D_{nn'}u_{n'} \ . \tag{4}$$

There are some general symmetries and constraints that must be obeyed by the force-constant matrix D. From the definition (3), it follows that the force-constant matrix D is real and symmetric

$$D_{nn'} = D_{n'n} \ . \tag{5a}$$

The translational symmetry of the lattice requires

$$D_{nn'} = D_{mm'} \quad \text{if} \quad t_n - t_{n'} = t_m - t_{m'} \ . \tag{5b}$$

Furthermore we have the general and important "sum rule"

$$\sum_{n'} D_{nn'} \equiv 0 \quad \text{for any } n \ ; \tag{5c}$$

this is a trivial consequence of the fact that the forces, given by Eq. (4), vanish not only when all nuclear displacements are zero, but also when all nuclear displacements are equal. Eq. (5a) and Eq. (5c) show that the sum of the matrix elements of any row or any column of the force-constant matrix D vanishes.

We consider now the classical equation of motion for the nth nucleus of mass M in the position $R_n = na + u_n$ under the force F_n; we have

$$\boxed{M\ddot{u}_n = -\sum_{n'} D_{nn'}u_{n'}} \tag{6}$$

with $n = 1, 2, \ldots, N$. The set of coupled differential equations (6) can be solved, in general, looking for solutions periodic in time of the form $u_n(t) = A_n \exp(-i\omega t)$. In the present case, we can take advantage of the translational symmetry of the force-constant matrix D in real space; this suggests to solve Eqs. (6) looking for solutions in the form of travelling waves, periodic in space and time, of the type

$$u_n(t) = A\, e^{i(qna-\omega t)} \,. \tag{7}$$

Replacing Eq. (7) into Eqs. (6), we have that the phonon frequencies ω are given by the relation

$$-M\omega^2 A = -\sum_{n'} D_{nn'}\, e^{-iq(na-n'a)} A \,.$$

The above expression can be recast in the form

$$\boxed{M\omega^2(q) = D(q)} \,, \tag{8a}$$

where

$$\boxed{D(q) = \sum_{n'} D_{nn'}\, e^{-iq(na-n'a)}} \,; \tag{8b}$$

notice that the Fourier transform $D(q)$ of the force-constant matrix elements $D_{nn'}$ does not depend on the specific value of n because of the property (5b).

Equation (8a) provides the dispersion relation $\omega = \omega(q)$ connecting the phonon frequency to the phonon wavenumber of the travelling plane wave of type (7). Notice that the displacements (7), are unaffected by changes of q by integer multiples of $2\pi/a$; the independent values of q are confined within the Brillouin zone $-\pi/a < q \leq \pi/a$. When standard Born–von Karman boundary conditions are applied, i.e. one requires $u_n(t) \equiv u_{n+N}(t)$, the allowed values of q within the Brillouin zone become discretized with values $m(2\pi/Na)$ and m integer; the number of allowed wavenumbers within the Brillouin zone equals the number of unit cells of the crystal (see Section I-1). We now apply our analysis to the specific case of a linear chain of atoms with nearest neighbour interactions only.

Linear monatomic chain with nearest neighbour interactions

To show the essential aspects of the lattice vibrations in the linear chain, we suppose that the only relevant inter-atomic interactions occur between nearest neighbour atoms; in other words, we assume that the only force constants different from zero are D_{nn}, $D_{n\,n+1}$ and $D_{n-1\,n}$. From the general properties of the force constants summarized by Eqs. (5), it is seen that there is a unique independent parameter (denoted below by C), and it holds

$$D_{nn} = 2C \,, \qquad D_{n\,n+1} = D_{n-1\,n} = -C \,. \tag{9}$$

The energy (2) of the linear chain, in the harmonic approximation and nearest

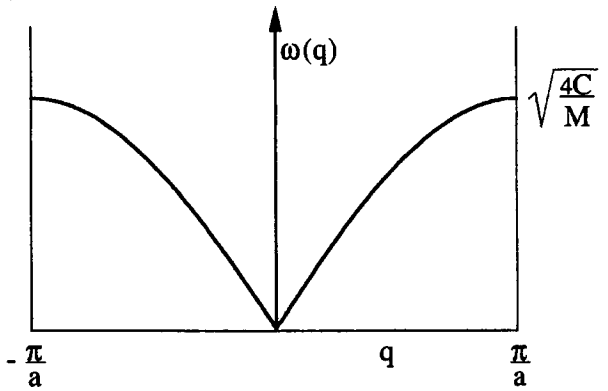

Fig. 2 Phonon dispersion curve for a monatomic linear lattice with nearest neighbour interactions only; the Brillouin zone is the segment between $-\pi/a$ and $+\pi/a$.

neighbour interaction becomes (taking $E_0(0)$ as the reference energy)

$$E_0^{(\mathrm{harm})} = \frac{1}{2}C\sum_n (2u_n^2 - u_n u_{n+1} - u_n u_{n-1}) \equiv \frac{1}{2}C\sum_n (u_n - u_{n+1})^2 \,. \tag{10}$$

Equation (10) is quite intuitive and represents the elastic energy of a chain of atoms, connected to nearest neighbours with springs of constant C.

The classical equations of motion (6) for the nuclear vibrations are thus

$$\boxed{M\ddot{u}_n = -C(2u_n - u_{n+1} - u_{n-1})} \tag{11}$$

for any n integer number. The set of discrete coupled differential equations (11) can be solved looking for travelling waves, periodic in space and time, of the form $u_n(t) = A\exp(iqna - i\omega t)$. By direct substitution, or equivalently from Eqs. (8), one obtains

$$-M\omega^2 = -C(2 - e^{iqa} - e^{-iqa}) = -4C\sin^2\frac{1}{2}qa \,. \tag{12a}$$

The dipersion relation for normal modes is thus

$$\omega = \sqrt{\frac{4C}{M}}\,|\sin\frac{1}{2}qa| \,, \tag{12b}$$

and is illustrated in Fig. 2; we see that the spectrum of vibrational frequencies extends from zero to a cutoff frequency $\omega_{\max} = \sqrt{4C/M}$.

It is interesting to consider the normal modes in the *long wavelength limit* $qa \ll 1$. The dispersion relation (12b) takes the form

$$\omega = \sqrt{\frac{C}{M}}\,aq \equiv v_s q \quad (qa \ll 1) \,;$$

the proportionality coefficient v_s between phonon frequency ω and phonon wavenum-

Table 1 Energy units of most frequent use for phonons.

	$h\nu\ (\nu = 10^{12}\,\text{hertz}) = 4.1357\,\text{meV}$	$\hbar\omega\ (\omega = 10^{13}\,\text{rad/sec}) = 6.5822\,\text{meV}$
	$1\,\text{eV}/hc = 8065\,\text{cm}^{-1}$	$1\,\text{eV}/\text{k}_B = 11605\,\text{K}$
for brevity:	$1\,\text{eV} \longleftrightarrow 8065\,\text{cm}^{-1}$	$1\,\text{eV} \longleftrightarrow 11605\,\text{K}$
	$1\,\text{meV} \longleftrightarrow 8.065\,\text{cm}^{-1}$	$1\,\text{cm}^{-1} \longleftrightarrow 0.124\,\text{meV}$

ber q represents the velocity of the sound in the medium, and is given by

$$v_s \equiv \sqrt{\frac{C}{M}}\, a\ . \tag{12c}$$

From Eq. (12c), we can estimate the value of the cutoff angular frequency

$$\omega_{\max} = 2\sqrt{\frac{C}{M}} = \frac{2v_s}{a} \approx \frac{10^5\,\text{cm/sec}}{10^{-8}\,\text{cm}} = 10^{13}\,\text{rad/sec}\ .$$

A typical vibration spectrum extends in general to the infrared region, up to energies $\hbar\omega$ of several tens of meV (see Table 1).

In the long wavelength limit, we can perform a continuous approximation to the set of discretized coupled differential equations (11); in fact $(-2u_n + u_{n+1} + u_{n-1})/a^2$ can be considered as the finite difference expression of the second order derivative $\partial^2 u/\partial x^2$. Equation (11) is thus equivalent to $M\ddot{u} = Ca^2\partial^2 u/\partial x^2$ and the propagation velocity of the elastic wave is again given by Eq. (12c).

2 Dynamics of diatomic one-dimensional lattices

We consider now the dynamics of a diatomic linear chain, of lattice constant a_0, with two atoms of mass M_1 and M_2 in the unit cell; this model can be considered as the prototype of a crystal with basis. In the equilibrium configuration, we assume that the atoms of mass M_1 occupy the sublattice positions $R_n^{(1)} = na_0$, while the atoms of mass M_2 occupy the sublattice positions $R_n^{(2)} = (n + 1/2)a_0$ (see Fig. 3).

We denote by u_n the displacements of the atoms of mass M_1 and with v_n the displacements of the atoms of mass M_2. For simplicity we assume that only nearest neighbour atoms interact with elastic forces of spring constant C. The classical equations of motion for the two types of particles are

$$\boxed{\begin{aligned} M_1\ddot{u}_n &= -C(2u_n - v_{n-1} - v_n) \\ M_2\ddot{v}_n &= -C(2v_n - u_n - u_{n+1}) \end{aligned}} \tag{13}$$

for any integer number n.

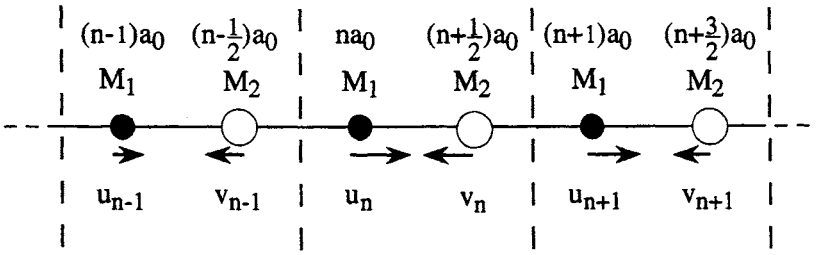

Fig. 3 Longitudinal displacements in a one-dimensional diatomic lattice. The equilibrium positions of the two sublattices of atoms, of mass M_1 and M_2, are indicated by black and white circles, respectively; the displacements u_n and v_n at a given instant are indicated by arrows.

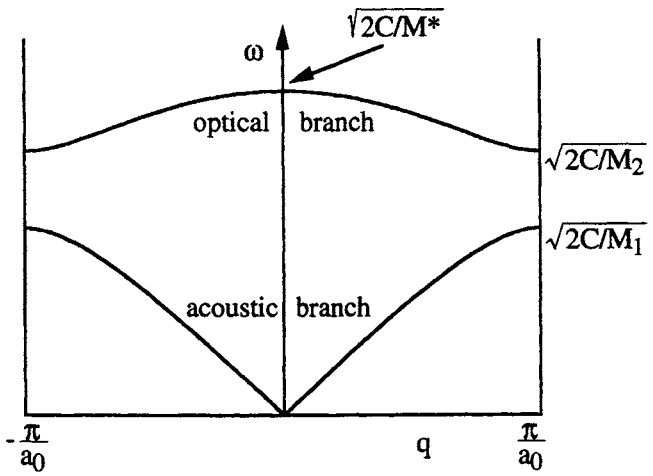

Fig. 4 Phonon dispersion curves of a diatomic linear chain, with nearest neighbour atoms interacting with spring constant C. The masses of the atoms are M_1 and M_2 (with $M_1 > M_2$); M^* is the reduced mass.

To solve the set of discrete coupled differential equations (13), we look for travelling waves, periodic in space and time, of the form

$$u_n(t) = A_1\, e^{i(qna_0-\omega t)} \quad \text{and} \quad v_n(t) = A_2\, e^{i(qna_0+qa_0/2-\omega t)}\,. \tag{14}$$

We notice that the vibrations of atoms of the same sublattice in different cells have the same amplitudes and phase relations of Bloch type.

Replacing (14) into (13), we obtain

$$-M_1\,\omega^2 A_1 = -C(2A_1 - A_2\, e^{-iqa_0/2} - A_2\, e^{iqa_0/2})$$

$$-M_2\,\omega^2 A_2 = -C(2A_2 - A_1\, e^{-iqa_0/2} - A_1\, e^{iqa_0/2})\,.$$

The two linear homogeneous equations in the two unknown amplitudes A_1 and A_2 have a non-trivial solution if the determinant of the coefficients of A_1 and A_2 is zero,

namely

$$\begin{vmatrix} 2C - M_1\omega^2 & -2C\cos\frac{qa_0}{2} \\ -2C\cos\frac{qa_0}{2} & 2C - M_2\omega^2 \end{vmatrix} = 0 .$$

The eigenvalues are given by

$$\omega^2 = C\left(\frac{1}{M_1} + \frac{1}{M_2}\right) \pm C\sqrt{\left(\frac{1}{M_1} + \frac{1}{M_2}\right)^2 - \frac{4\sin^2(qa_0/2)}{M_1 M_2}} , \tag{15a}$$

and the corresponding amplitudes satisfy the relation

$$\frac{A_1}{A_2} = \frac{2C\cos(qa_0/2)}{2C - M_1\omega^2} . \tag{15b}$$

The dispersion relations (15a) are illustrated in Fig. 4. We have now two branches, the lower one called "acoustic" and the upper one called "optical", with a frequency gap between them. In the particular case that $M_1 \equiv M_2$, the gap between the acoustic branch and the optical branch disappears and we recover the result of the previous section [in the case $M_1 \equiv M_2$, Fig. 4 and Fig. 2 coincide exactly, once the trivial folding due to the fact that $a_0 = 2a$ is performed].

Long wavelength limit of a diatomic linear chain: acoustic and optical modes

We consider now the normal modes of a diatomic chain in the long wavelength limit $qa_0 \ll 1$. For small qa_0, the two roots ω^2 and the corresponding amplitudes (given by Eqs. 15) are

$$\omega^2 = \frac{2C}{M_1 + M_2}\left(\frac{a_0}{2}\right)^2 q^2 + O(q^4) \qquad A_1 = A_2 \quad \text{acoustic branch}$$

and

$$\omega^2 = \frac{2C}{M^*} + O(q^2) \qquad M_1 A_1 = -M_2 A_2 \quad \text{optical branch} ,$$

where M^* is the reduced mass given by $1/M^* = (1/M_1) + (1/M_2)$.

In the acoustic branch, in the long wavelength limit, the atoms vibrate in phase and with the same amplitude; the frequency ω is proportional to the wavenumber q, and the proportionality coefficient, the sound velocity v_s, is given by

$$v_s = \sqrt{\frac{C}{(M_1 + M_2)/2}}\,\frac{a_0}{2} .$$

The above relation is the obvious counterpart of expression (12c), if we notice that the average mass $(M_1 + M_2)/2$ replaces the mass M; a and $a_0/2$ denote nearest neighbour distance in the monatomic and diatomic models, respectively; C is the spring constant.

In the upper branch, A_1 and A_2 have opposite signs and absolute values inversely proportional to atomic masses; this means that the two atoms in the unit cell move in opposite directions, while the "center of mass" of the unit cell remains fixed. As $q \to 0$, the frequency $\omega(q)$ of the optical branch tends to the finite value $\omega_0 = \sqrt{2C/M^*}$.

It is instructive to consider the optical modes of the diatomic chain in the continuous approximation; this is useful also to justify the origin of the name attached to such a branch. For optical modes in the long wavelength limit, we can assume that nearest neighbour atoms on the same sublattice have the same displacements. Eqs. (13) can be recast in the form

$$M_1\ddot{u} = -2C(u-v) \tag{16a}$$

$$M_2\ddot{v} = -2C(v-u)\ , \tag{16b}$$

where the discretized index n is now replaced by the continuous variable x in the argument of the functions $u(x,t)$ and $v(x,t)$. In optical modes, the atoms in the two sublattices move against each other; so it is convenient to discuss optical vibrations via the *relative displacement variable* $w = u - v$. If we divide both members of Eq. (16a) by M_1, both members of Eq. (16b) by M_2, and subtract, we obtain

$$\ddot{w} = -\omega_0^2 w \tag{17}$$

where $\omega_0 = \sqrt{2C/M^*}$; the relative motion of the atoms M_1 and M_2 around the center of mass of the unit cell is harmonic with frequency ω_0.

The optical modes owe their name to the fact that they are expected to couple strongly with electromagnetic fields (of appropriate frequency). Suppose in fact that the diatomic crystal can be pictured as composed by ionic (or partially ionic) units, with effective net charge $\pm e^*$ (*polar crystals*). In the presence of electric fields, the equations of motion (16) have to be modified in the form

$$M_1\ddot{u} = -2C(u-v) + e^*E_{\text{loc}} \tag{18a}$$

$$M_2\ddot{v} = -2C(v-u) - e^*E_{\text{loc}}\ . \tag{18b}$$

We have indicated with E_{loc} the local electric field acting at the lattice sites, as this field may be different from the average macroscopic electromagnetic field; the distinction between local and average fields (if any) is discussed in Section 7-3. In terms of the relative displacement w we have

$$\ddot{w} = -\omega_0^2 w + \frac{e^*}{M^*}E_{\text{loc}}\ ; \tag{19}$$

the above equation describes the forced oscillations of a mechanical system of proper frequency ω_0, coupled to a driving field of some frequency ω; coupling effects are expected to be particularly significant when the frequency ω is resonant or almost resonant with the optical mode frequency ω_0. A detailed analysis of the coupling of photon and phonon modes in polar crystals, and the resulting polariton effects are discussed in Section 7.

3 Dynamics of general three-dimensional crystals

Crystal dynamical matrix and phonon frequencies

In the previous two sections, we have discussed the lattice dynamics of one-dimensional crystals, with or without a basis. We complete now the subject, addressing the general

problem of lattice dynamics of three-dimensional crystals, with or without a basis; for this purpose, we follow step-by-step the script of the previous two sections.

Consider a general three-dimensional crystal, with N unit cells, translational vectors $\mathbf{t}_n$, and a basis of atoms in the positions $\mathbf{d}_1$, $\mathbf{d}_2$, ..., $\mathbf{d}_{n_b}$. We label atoms with two indices $(n\nu)$, where the (Latin) index n denotes the unit cells of the crystal and the (Greek) index ν the atoms inside the unit cell. According to the general principles of the adiabatic approximation, we consider first *the nuclei fixed in the positions* $\mathbf{t}_n + \mathbf{d}_\nu + \mathbf{u}_{n\nu}$, and we denote by $E_0(\{\mathbf{u}_{n\nu}\})$ the total ground-state energy (or *static lattice energy*) of the electronic-nuclear system. The expansion of E_0 up to second order in the displacements from the equilibrium positions (*harmonic approximation*) gives

$$E_0^{(\mathrm{harm})}(\{\mathbf{u}_{n\nu}\}) = E_0(0) + \frac{1}{2} \sum_{n\nu\alpha, n'\nu'\alpha'} D_{n\nu\alpha,n'\nu'\alpha'} u_{n\nu\alpha} u_{n'\nu'\alpha'} \tag{20a}$$

where $\alpha, \alpha' = x, y, z$; $\nu, \nu' = 1, 2, \ldots, n_b$; $n = 1, 2, \ldots, N$. The "force constants" are defined as the second derivative of $E_0(\{\mathbf{u}_{n\nu}\})$ evaluated at the equilibrium configuration

$$D_{n\nu\alpha,n'\nu'\alpha'} = \left(\frac{\partial^2 E_0}{\partial u_{n\nu\alpha}\, \partial u_{n'\nu'\alpha'}} \right)_0 . \tag{20b}$$

In the expansion (20a), the linear terms in the displacements are not present since $\partial E_0 / \partial u_{n\nu\alpha} \equiv 0$ at the equilibrium configuration.

The matrix D, formed with the "force constants" elements $D_{n\nu\alpha,n'\nu'\alpha'}$, obeys some general properties and constraints. From the definition (20b), we have immediately that the matrix D is real and symmetric, with

$$D_{n\nu\alpha,n'\nu'\alpha'} = D_{n'\nu'\alpha',n\nu\alpha} . \tag{21a}$$

The translation symmetry of the lattice implies

$$D_{n\nu\alpha,n'\nu'\alpha'} = D_{m\nu\alpha,m'\nu'\alpha'} \quad \text{if} \quad \mathbf{t}_n - \mathbf{t}_{n'} = \mathbf{t}_m - \mathbf{t}_{m'} ; \tag{21b}$$

(the presence of point symmetry operations may imply further constraints, that can be analysed with group theory considerations). Furthermore we have the general and important "sum rule"

$$\sum_{n'\nu'} D_{n\nu\alpha,n'\nu'\alpha'} \equiv 0 \tag{21c}$$

[the proof is a straightforward generalization of what already done for the demonstration of Eq. (5c)].

The classical equations of motion for the nuclei in the instantaneous positions $\mathbf{t}_n + \mathbf{d}_\nu + \mathbf{u}_{n\nu}$ under the forces $\mathbf{F}_{n\nu} = -\partial E_0^{(\mathrm{harm})} / \partial \mathbf{u}_{n\nu}$ are

$$\boxed{M_\nu \ddot{u}_{n\nu\alpha} = - \sum_{n'\nu'\alpha'} D_{n\nu\alpha,n'\nu'\alpha'}\, u_{n'\nu'\alpha'}} \tag{22}$$

where $n, n' = 1, 2, \ldots, N$; $\nu, \nu' = 1, 2, \ldots, n_b$; $\alpha, \alpha' = x, y, z$. The presence of translational symmetry suggests to solve the set of coupled differential equations (22) looking for solutions in the form of travelling waves of the type

$$\mathbf{u}_{n\nu}(t) = \mathbf{A}_\nu(\mathbf{q}, \omega)\, e^{i(\mathbf{q}\cdot\mathbf{t}_n - \omega t)} \,. \tag{23a}$$

The *polarization vectors* $A_{\nu\alpha}(\mathbf{q}, \omega)$ ($\nu = 1, 2, \ldots, n_b$; $\alpha = x, y, z$) of the vibrations of the nuclei within the primitive cell are left unspecified and are determined below by solution of an appropriate secular equation. Replacing (23a) into (22), we have

$$-M_\nu \omega^2 A_{\nu\alpha} = -\sum_{n'\nu'\alpha'} D_{n\nu\alpha, n'\nu'\alpha'}\, e^{-i\mathbf{q}\cdot(\mathbf{t}_n - \mathbf{t}_{n'})} A_{\nu'\alpha'} \,. \tag{23b}$$

Non trivial solutions of Eq. (23b) are obtained by solving the determinantal equation

$$\boxed{\left\| D_{\nu\alpha,\nu'\alpha'}(\mathbf{q}) - M_\nu \omega^2 \delta_{\alpha\alpha'} \delta_{\nu,\nu'} \right\| = 0} \,, \tag{23c}$$

where

$$\boxed{D_{\nu\alpha,\nu'\alpha'}(\mathbf{q}) = \sum_{n'} D_{n\nu\alpha,n'\nu'\alpha'}\, e^{-i\mathbf{q}\cdot(\mathbf{t}_n - \mathbf{t}_{n'})}} \,. \tag{23d}$$

The matrix $D(\mathbf{q})$, with elements $D_{\nu\alpha,\nu'\alpha'}(\mathbf{q})$ is called "*the dynamical matrix of the crystal*" in reciprocal space.

Equation (23c) is the fundamental eigenvalue equation for the normal modes of a crystal. The dynamical matrix $D(\mathbf{q})$ has dimension $3n_b$, where n_b is the number of atoms forming the basis of the unit cell. The secular equation (23c) produces $3n_b$ eigenvalues (called phonons or normal modes); at every vector $\mathbf{q}$ we have thus $3n_b$ normal modes, giving rise to $3n_b$ phonon branches as $\mathbf{q}$ is varied within the first Brillouin zone. For a crystal with N unit cells, the total number of normal modes equals $3n_bN$, i.e. 3 times the total number of atoms. Let $\omega(\mathbf{q}, p)$ ($p = 1, 2, \ldots 3n_b$) denote the frequency of the p-th normal mode of wavevector $\mathbf{q}$, and $\mathbf{A}_\nu(\mathbf{q}, p)$ ($\nu = 1, 2, \ldots, n_b$) the corresponding polarization vectors. A mode $\omega(\mathbf{q}, p)$ is called "longitudinal" (or "transverse") in the case the polarization vectors $\mathbf{A}_\nu(\mathbf{q}, p)$ are parallel to $\mathbf{q}$ (or perpendicular to $\mathbf{q}$). Modes which involve oscillating electric dipoles are called "optically active" since they can couple directly with electromagnetic fields.

From the standard algebraic properties of matrix eigenvalue equations, the eigenvectors of the secular equation (23c) satisfy the orthogonality relations

$$\sum_{\nu\alpha} M_\nu A^*_{\nu\alpha}(\mathbf{q}, p)\, A_{\nu\alpha}(\mathbf{q}, p') = \delta_{p,p'} \,.$$

The above relation can be written in extended form

$$M_1 \mathbf{A}^*_1(\mathbf{q}, p) \cdot \mathbf{A}_1(\mathbf{q}, p') + \ldots + M_{n_b} \mathbf{A}^*_{n_b}(\mathbf{q}, p) \cdot \mathbf{A}_{n_b}(\mathbf{q}, p') = \delta_{p,p'} \,. \tag{24}$$

In the case of a monatomic three-dimensional Bravais lattice, $n_b = 1$ in Eq. (24), and for the three branches it holds $\mathbf{A}^*(\mathbf{q}, p) \cdot \mathbf{A}(\mathbf{q}, p') = \delta_{p,p'}$.

It is interesting to consider the eigenvalue equation (23c) in the long wavelength limit $\mathbf{q} \to 0$. From the sum rule (21c) and Eq. (23d) it follows

$$\sum_{\nu'} D_{\nu\alpha,\nu'\alpha'}(\mathbf{q}=0) \equiv 0 \ ;$$

in particular we have

$$\sum_{\nu'\alpha'} D_{\nu\alpha,\nu'\alpha'}(\mathbf{q}=0)\, A_{\alpha'} \equiv 0 \ . \tag{25a}$$

The above equation shows that vibrations, with amplitudes $A_{\nu'\alpha'} \equiv A_{\alpha'}$ equal for all the atoms of the basis, satisfy the secular equation (23c) with frequency $\omega = 0$. Thus *any three-dimensional crystal presents three acoustic branches* with $\omega(\mathbf{q}) \to 0$ as $\mathbf{q} \to 0$, with all atoms in the unit cell vibrating in phase and with the same amplitude. The remaining $3n_b - 3$ "optical" modes vibrate in such a way that the motion of the center of mass of the cell is unaltered; in fact the orthogonality relation (24) to the acoustic modes, with polarization vectors $\mathbf{A}^*$ independent from the atomic index, gives

$$M_1\mathbf{A}_1 + M_2\mathbf{A}_2 + \ldots + M_{n_b}\mathbf{A}_{n_b} = 0 \tag{25b}$$

for any of the optical modes.

Before considering a few examples of phonon branches in crystals, it is convenient to summarize the basic approximations contained in the dynamical matrix approach. According to the general adiabatic principle (see Section VIII-2), one preliminarily considers the nuclei fixed in a given configuration $\{R_I\}$, and determines (ab initio or semiempirically) the total ground-state energy $E_0(\{R_I\})$ versus $\{R_I\}$ (the ground state is supposed to be non-degenerate). Then, the crucial assumption is done that the static lattice energy $E_0(\{R_I\})$, which is just a static property, actually controls the nuclear dynamics. To justify this crucial point, it is required that transitions from the ground adiabatic surface to the excited adiabatic surfaces, induced by the nuclear motion, can be neglected. It is also required that the forces acting on the nuclei depend on the instantaneous nuclear positions, so that retardation effects can be neglected too. Finally, it is assumed that the displacements from equilibrium positions are sufficiently small to justify the expansion of $E_0(\{R_I\})$ to second order in the displacements. In summary, the basic approximations of the crystal dynamical matrix approach include (*i*) *the adiabatic approximation*, (*ii*) *the harmonic approximation*, and (*iii*) *instantly interparticle interactions.*

Phonon dispersion curves with the crystal dynamical matrix and short-range or long-range nature of force constants

We wish now to provide a few illustrative examples of phonon dispersion curves in crystals, obtained with the force constant approach. First principle methods based on the density functional theory have permitted the accurate calculation of the total ground-state energy of several materials (with the nuclei fixed in chosen configurations); this has made it possible the more ambitious project of calculating the inter-atomic force constants in a number of cases. First principle calculations of force constants are in

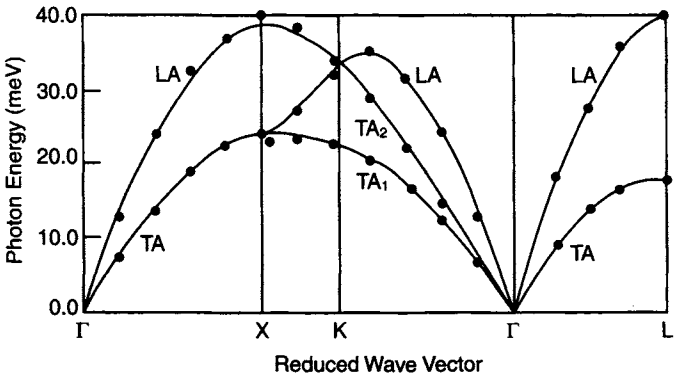

Fig. 5 Phonon dispersion curves of aluminum along symmetry directions. The solid lines represents the calculations of A. A. Quong and B. M. Klein, Phys. Rev. B**46**, 10734 (1992) (copyright 1992 by the American Physical Society). Longitudinal and transverse acoustic branches are indicated by LA and TA (or TA_1 and TA_2), respectively. The experimental points are from the papers of G. Gilat and R. M. Nicklow, Phys. Rev. **143**, 487 (1966) and R. Stedman, S. Almqvist and G. Nilsson, Phys. Rev. **162**, 549 (1967).

general very demanding; thus most often, empirical assumptions and special models of interaction are made. The assumption of "two-body" central forces, acting between pairs of atoms composing the lattice is the most common; however in many cases this approximation is too drastic, and angular forces and torsional forces are to be included appropriately. Often the force constants of the dynamical matrix are considered as disposable or semi-empirical parameters.

Once a specific model of interatomic forces has been chosen, the dynamical matrix in reciprocal space can be set up and diagonalization at several points of the Brillouin zone provides the phonon dispersion curves of the crystal. Some crystals can be intuitively described as consisting of neutral atoms interacting with *short-range forces*; the force constants extend to a reasonably small number of shells (say nearest neighbours, second nearest neighbours and possibly a few more up to ten shells or so) and become safely negligible afterwards. Examples of crystals with short-range nature of inter-atomic forces include simple Bravais lattices, metals, homopolar elemental semiconductors (such as silicon and germanium).

In polar crystals, such as ionic crystals and heteropolar semiconductors, the crystal lattice can be intuitively described as constituted by charged ions interacting both with *short-range forces and long-range Coulomb forces.* In the ionic picture of polar crystals, appropriate site dependent "Born effective charges" are attributed to the ions of the different sublattices, to mimic long-range interactions.

The crystal dynamical matrix for polar crystals is obtained by direct summation of short-range terms and Ewald method for long-range Coulomb terms. It should be noticed that the dynamical matrix of polar crystals at small q is particularly vulnerable to the long-range nature of the force constants in real space; actually, the dynamical

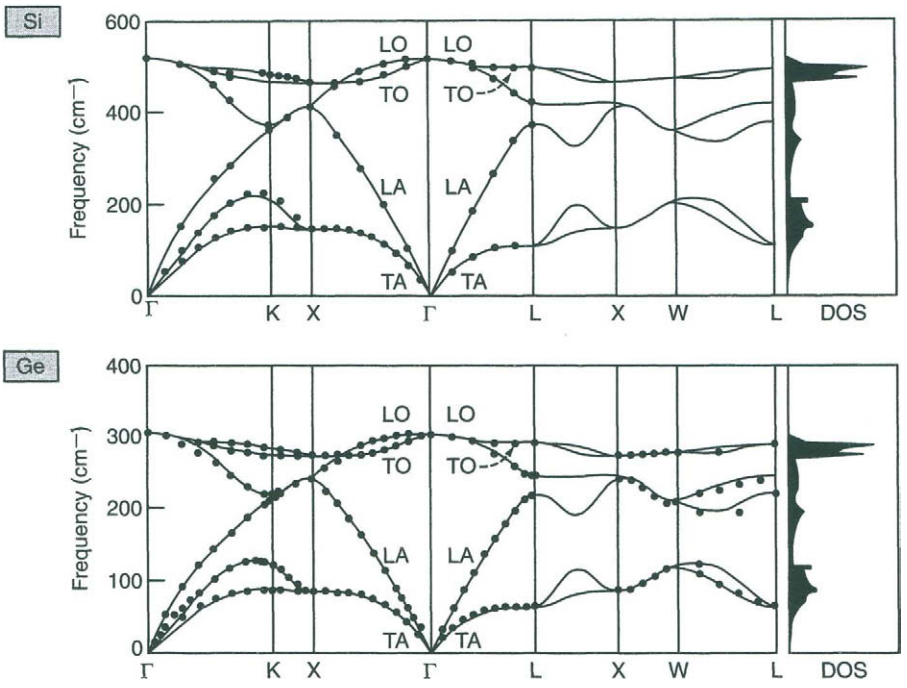

Fig. 6 Phonon dispersion curves and density-of-states of Si and Ge calculated by P. Giannozzi, S. de Gironcoli, P. Pavone and S. Baroni, Phys. Rev. B**43**, 7231 (1991) (copyright 1991 by the American Physical Society). Longitudinal and transverse acoustic (or optical) modes are indicated by LA and TA (LO and TO), respectively. The experimental points are from G. Dolling, in "Inelastic Scattering of Neutrons in Solids and Liquids" edited by S. Ekland (IAEA, Vienna 1963) Vol.II, p.37; G. Nilsson and G. Nelin, Phys. Rev. B**3**, 364 (1971) and Phys. Rev. B**6**, 3777 (1972). Conversion to meV units can be done noting that 1 cm^{-1}= 0.124 meV.

matrix has a pathological behaviour (called "non-analyticity"), which is responsible of the transverse-longitudinal splitting of optical phonons (see Section 7 for further aspects). The effects due to the long-range nature of inter-atomic forces are evident in the optical phonon branches of polar semiconductors (see Fig. 7), and are even more important in typical ionic crystals (see Fig. 8).

In Fig. 5 we show the phonon dispersion curves of aluminum, together with the experimental measurements obtained with coherent inelastic scattering of slow neutrons. Since aluminum crystallizes in a simple fcc Bravais lattice, the phonon dipersion curves consist of three acoustic branches. The acoustic modes are degenerate at $\mathbf{q} = 0$; along the high symmetry directions ΓL and ΓX the two transverse modes are degenerate; in directions of low or no symmetry, the three branches are non-degenerate.

In Fig. 6 we show the phonon dispersion curves of silicon and germanium. Since these elemental semiconductors crystallize in a fcc lattice with two atoms per unit cell, we have now three acoustic branches and three optical branches. The acoustic

Table 2 Frequencies ω_{LO} and ω_{TO} (in cm^{-1}) of longitudinal optical and transverse optical phonons for six semiconductors. The calculations are taken from P. Giannozzi, S. de Gironcoli, P. Pavone and S. Baroni, Phys. Rev. B**43**, 7231 (1991), to which we refer for further details; experimental data are in parentheses. The static and the high frequency dielectric constants are also given; notice that the ratio $\omega_{LO}^2/\omega_{TO}^2$ equals (within experimental error) the ratio $\varepsilon_s/\varepsilon_\infty$.

	Si	Ge	GaAs	AlAs	GaSb	AlSb
ω_{LO}	517 (517)	306 (304)	291 (291)	400 (402)	237 (233)	334 (344)
ω_{TO}	517 (517)	306 (304)	271 (271)	363 (361)	230 (224)	316 (323)
$\frac{\omega_{LO}^2}{\omega_{TO}^2}$	1	1	1.15 (1.17)	1.22 (1.24)	1.06 (1.08)	1.12 (1.14)
ε_s	12.1	16.5	12.40	10.06	15.69	12.04
ε_∞	12.1	16.5	10.60	8.16	14.44	10.24
$\frac{\varepsilon_s}{\varepsilon_\infty}$	1	1	1.17	1.23	1.09	1.17

branches as well as the optical branches are degenerate at $\mathbf{q} = 0$. Along the high symmetry directions ΓX and ΓL the two transverse acoustic modes and the two transverse optical modes are degenerate; in direction of low or no symmetry, all modes are non-degenerate.

In Fig. 7 we show the phonon dispersion curves for heteropolar semiconductors GaAs, AlAs, GaSb and AlSb. In these crystals the inter-atomic forces include long-range Coulomb interaction, because of the partial ionic nature of the chemical bond. Since these heteropolar semiconductors crystallize in a fcc lattice with two atoms per unit cell, the phonon curves present three acoustic and three optical branches; as expected, the acoustic and optical branches are well separated in crystals where the mass difference of the two atoms in the unit cell is large. A most important feature of Fig. 7 is the longitudinal-transverse splitting of optical modes at $\mathbf{q} \approx 0$; this splitting is the fingerprint of the long-range nature of inter-atomic forces, and is connected with the break of cubic symmetry, due to the induced dipoles accompanying the vibrational modes. A simplified modellistic study of the long-wavelength optical phonons is given in Section 7. In Table 2 we report for convenience the frequencies of the optical phonons at the center of the Brillouin zone for the elemental semiconductors Si and Ge, and for the polar semiconductors GaAs, AlAs, GaSb, AlSb.

As a final example, we report in Fig. 8 the phonon branches of LiF. Lithium fluoride is a typical ionic material with the NaCl structure; there are two ions in the unit cell, and there are thus three acoustic and three optical branches. The long-range nature of interionic forces produces a strong longitudinal-transverse splitting of optical modes at $\mathbf{q} \approx 0$. In LiF the ratio of the low-frequency dielectric constant ($\varepsilon_s = 8.9$) and high-frequency dielectric constant ($\varepsilon_\infty = 1.9$) is relatively large, and so is the squared ratio of the measured LO and TO mode frequencies.

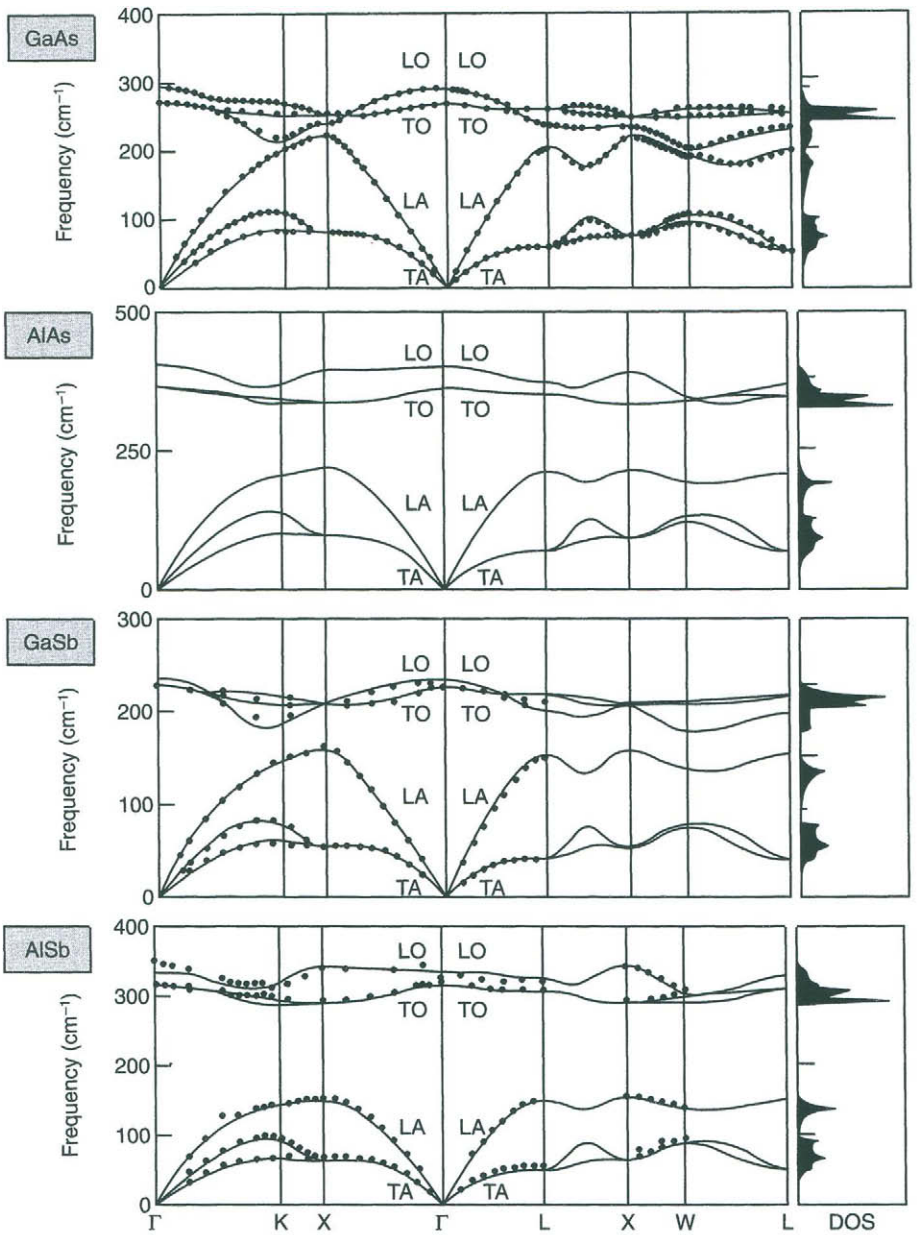

Fig. 7 Calculated phonon dispersion curves and density-of-states for binary semiconductors GaAs, AlAs, GaSb and AlSb [from P. Giannozzi, S. de Gironcoli, P. Pavone and S. Baroni, Phys. Rev. B**43**, 7231 (1991); copyright 1991 by the American Physical Society]. Longitudinal and transverse acoustic (or optical) modes are indicated by LA and TA (LO and TO), respectively.

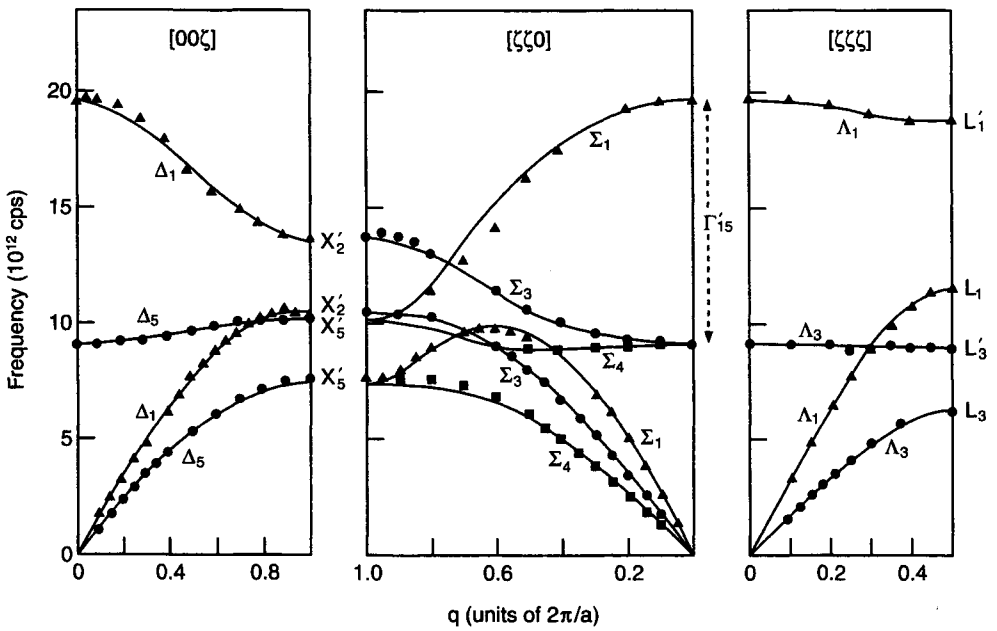

Fig. 8 Measured phonon dispersion curves along three directions of high symmetry in LiF; the solid curves are a best least-squares fit of a parameter model [from G. Dolling, H. G. Smith, R. M. Nicklow, P. R. Vijayaraghavan and M. K. Wilkinson, Phys. Rev. **168**, 970 (1968); copyright 1968 by the American Physical Society].

4 Quantum theory of the harmonic crystal

In the previous sections, we have discussed the lattice vibrations by means of the classical equations of motion. We can reconsider the problem from a quantum mechanical point of view, and show that the classical and quantum treatments are completely equivalent as far as dispersion curves are concerned; on the other hand, the quantum treatment of the elastic field shows that energies are discretized into quanta, called phonons.

In Section 1, we have considered the classical dynamics of a monatomic linear chain; we consider now the quantum mechanical counterpart of the same problem. In the harmonic approximation, and nearest neighbour interactions (see Eq. 10), the Hamiltonian of the linear chain becomes

$$H = \sum_n \frac{1}{2M} p_n^2 + \frac{1}{2} C \sum_n (2u_n^2 - u_n u_{n+1} - u_n u_{n-1}) \,, \tag{26}$$

where u_n and p_n are the coordinate and conjugate moment of the nucleus at the nth site; these observables obey the commutation rules

$$[u_n, p_{n'}] = i\hbar\delta_{n,n'} \,, \qquad [u_n, u_{n'}] = [p_n, p_{n'}] = 0 \,. \tag{27}$$

Instead of the dynamical variables u_n and p_n, it is convenient to perform a canonical

transformation, with the final aim to put in diagonal form the Hamiltonian (26). We define the "phonon annihilation operator" a_q and the "phonon creation operator" $a_q^\dagger$ as the following linear combination of displacements and momenta of the nuclei

$$a_q = \frac{1}{\sqrt{N}} \sum_{t_n} e^{-iqt_n} \left[\sqrt{\frac{M\omega(q)}{2\hbar}}\, u_n + i \sqrt{\frac{1}{2\hbar M\omega(q)}}\, p_n \right] \tag{28a}$$

$$a_q^\dagger = \frac{1}{\sqrt{N}} \sum_{t_n} e^{iqt_n} \left[\sqrt{\frac{M\omega(q)}{2\hbar}}\, u_n - i \sqrt{\frac{1}{2\hbar M\omega(q)}}\, p_n \right] . \tag{28b}$$

The angular frequency $\omega(q)$ is at the moment left unspecified, and determined later so that to diagonalize the operator H. According to Eqs. (28), the phonon annihilation and creation operators are defined as linear combinations of the dynamical variables of all the nuclei, with appropriate phase factors $\exp(iqt_n)$ of the Bloch form.

It is easily seen that the transformations (28) from the set of operators u_n, p_n, to the set of operators a_q, $a_q^\dagger$ are canonical, i.e. the commutation rules are preserved. For this purpose we remember the standard properties

$$\frac{1}{N} \sum_{t_n} e^{-i(q-q')t_n} = \delta_{q,q'} \qquad \text{and} \qquad \frac{1}{N} \sum_{q} e^{-iq(t_n - t_{n'})} = \delta_{n,n'} . \tag{29}$$

From the first of relations (29) and commutation rules (27), it is immediate to verify that

$$\left[a_q, a_{q'}^\dagger\right] = \delta_{q,q'} \quad \text{and} \quad \left[a_q, a_{q'}\right] = \left[a_q^\dagger, a_{q'}^\dagger\right] = 0 ;$$

thus the transformation (28) is canonical.

With the use of the second of the relations (29), we can invert Eqs. (28) and obtain

$$u_n = \frac{1}{\sqrt{N}} \sum_{q} \sqrt{\frac{\hbar}{2M\omega(q)}}\, e^{iqt_n} \left[a_q + a_{-q}^\dagger\right] \tag{30a}$$

$$p_n = \frac{-i}{\sqrt{N}} \sum_{q} \sqrt{\frac{\hbar M\omega(q)}{2}}\, e^{iqt_n} \left[a_q - a_{-q}^\dagger\right] . \tag{30b}$$

Insertion of Eqs. (30) into Eq. (26) gives

$$\begin{aligned} H = &- \frac{1}{4} \sum_{q} \hbar\omega(q) \left[a_q - a_{-q}^\dagger\right] \left[a_{-q} - a_q^\dagger\right] \\ &+ \frac{1}{4} \sum_{q} \frac{\hbar}{\omega(q)} \frac{C}{M} \left[a_q + a_{-q}^\dagger\right] \left[a_{-q} + a_q^\dagger\right] \left[2 - e^{iqa} - e^{-iqa}\right] . \end{aligned}$$

We now exploit the arbitrariness in the frequency $\omega(q)$ by choosing

$$\boxed{\omega(q) = \frac{1}{\omega(q)} \frac{C}{M} (2 - e^{iqa} - e^{-iqa})} ; \tag{31a}$$

notice the equivalence of Eq. (31a) and Eq. (12). The Hamiltonian (26) of the linear chain then becomes

$$\boxed{H = \sum_q \hbar\omega(q)(a_q^\dagger a_q + \frac{1}{2})}\,, \tag{31b}$$

which is the sum of the Hamiltonians of N independent linear oscillators of frequency $\omega(q)$. The quanta of energy $\hbar\omega(q)$ are called phonons.

Completely similar analysis and conclusions could be performed for the diatomic linear chain of Section 2, and the general three-dimensional crystal of Section 3; the dispersion relations provided by the quantum mechanical treatment and by the classical treatment are the same, since the unitary transformation from localized variables to itinerant (or collective) variables are the same in the classical and quantum treatment. The quantum theory thus recovers the same $\omega = \omega(\mathbf{q}, p)$ dispersion curves of the classical theory; however the quantum theory leads to the quantization of the elastic field in terms of phonons, which can be considered as travelling quanta of energy $\hbar\omega = \hbar\omega(\mathbf{q}, p)$, wavevector propagation $\mathbf{q}$ and branch index p ($p = 1, 2, \ldots 3n_b$).

5 Lattice heat capacity. Einstein and Debye models

Consider a crystal composed by N unit cells and a basis of n_b atoms in the unit cell; the crystal volume is $V = N\Omega$ and the total number of atoms is $N_a = N\, n_b$. In the harmonic approximation, the system of N_a vibrating atoms is equivalent to a system of $3N_a$ independent (one-dimensional) oscillators of frequency $\omega = \omega(\mathbf{q}, p)$, where $\mathbf{q}$ assumes N allowed values in the first Brillouin zone, and p runs over the $3n_b$ branches of the phonon dispersion curves. The average vibrational energy of the harmonic crystal is the sum of independent phonon contributions; according to the Bose–Einstein statistics, we have

$$U_{\text{vibr}}(T) = \sum_{\mathbf{q}\,p} \left[\frac{\hbar\omega(\mathbf{q}, p)}{e^{\hbar\omega(\mathbf{q},p)/k_B T} - 1} + \frac{1}{2}\hbar\omega(\mathbf{q}, p) \right] .$$

The *lattice heat capacity at constant volume*, using Eq. (III-23a), is given by

$$\boxed{C_V(T) = \frac{\partial U_{\text{vibr}}}{\partial T} = \frac{\partial}{\partial T} \sum_{\mathbf{q}\,p} \frac{\hbar\omega(\mathbf{q}, p)}{e^{\hbar\omega(\mathbf{q},p)/k_B T} - 1}}\,. \tag{32}$$

The above expression allows the numerical calculation of the lattice heat capacity of crystals, once the phonon dispersion curves $\omega(\mathbf{q}, p)$ are known. In the following we consider the application of Eq. (32) to simple models of dispersion curves, that can be worked out analytically.

Einstein model

In the Einstein model, the actual frequencies of the normal modes are replaced by a unique (average) frequency ω_e (Einstein frequency). If N_a is the total number of

atoms, Eq. (32) for the heat capacity at constant volume becomes

$$C_V(T) = 3N_a \frac{\partial}{\partial T} \frac{\hbar\omega_e}{e^{\hbar\omega_e/k_BT} - 1} = 3N_a k_B \left(\frac{\hbar\omega_e}{k_BT}\right)^2 \frac{e^{\hbar\omega_e/k_BT}}{(e^{\hbar\omega_e/k_BT} - 1)^2} .$$

The behaviour of $C_V(T)$ in the low and high temperature limits is

$$C_V \to e^{-\hbar\omega_e/k_BT} \quad \text{for} \quad k_BT \ll \hbar\omega_e ,$$

and

$$C_V \to 3N_a k_B \quad \text{for} \quad k_BT \gg \hbar\omega_e .$$

In the high temperature limit the Einstein model recovers the Dulong and Petit value $3N_a k_B$. In the low temperature limit, the Einstein model predicts for $C_V(T)$ an exponentially vanishing behaviour, contrary to the T^3 experimental law. The origin of this discrepancy is the presence in crystals of the phonon acoustic branches, which cannot be mimicked by a unique Einstein frequency, and actually need a more realistic description.

Debye model

Any three-dimensional crystal, with or without a basis, presents three acoustic branches with linear dispersion $\omega = v_s q$ for small q. For simplicity we assume the same sound velocity v_s for each of the three acoustic branches and extend the linear dispersion relation to the whole Brillouin zone. To avoid inessential details, we approximate the Brillouin zone with a sphere (Debye sphere) of equal volume (in order to preserve the total number of allowed wavevectors); we indicate with q_D the radius of the Debye sphere and define $\omega_D = v_s q_D$ as the *cutoff Debye frequency.* We notice that $(4/3)\pi q_D^3 = (2\pi)^3/\Omega$, where Ω is the volume of the unit cell in the direct space.

The density of phonon states corresponding to a branch with linear dispersion relation $\omega = v_s q$ is easily obtained. In fact the number of states $D(\omega)\, d\omega$ with frequency in the interval $[\omega\,, \omega + d\omega]$ equals the number of states in the reciprocal space with wavevector between $[q\,, q + dq]$; namely:

$$D(\omega)\, d\omega = \frac{V}{(2\pi)^3} 4\pi q^2 dq = \frac{V}{(2\pi)^3} 4\pi \left(\frac{\omega}{v_s}\right)^2 d\frac{\omega}{v_s} .$$

It follows

$$D(\omega) = \frac{V}{(2\pi)^3} 4\pi \frac{\omega^2}{v_s^3} = \frac{N\Omega}{(2\pi)^3} \frac{4\pi q_D^3}{3} \frac{3\omega^2}{\omega_D^3} = N \frac{3\omega^2}{\omega_D^3} \qquad 0 \le \omega \le \omega_D \tag{33}$$

(N is the number of unit cells of the crystal).

The contribution of the three acoustic branches to the average vibrational energy (apart the constant zero point energy) is

$$U_{\text{vibr}}^{(\text{acoustic})}(T) = 3 \int_0^{\omega_D} N \frac{3\omega^2}{\omega_D^3} \frac{\hbar\omega}{e^{\hbar\omega/k_BT} - 1}\, d\omega . \tag{34}$$

It is convenient to perform the change of variables $x = \hbar\omega/k_BT$ and define $x_D =$

$\hbar\omega_D/k_BT = T_D/T$, where $T_D = \hbar\omega_D/k_B$ is called Debye temperature. The expression (34) becomes

$$U_{\text{vibr}}^{(\text{acoustic})}(T) = 9Nk_BT\left(\frac{T}{T_D}\right)^3 \int_0^{x_D} \frac{x^3}{e^x - 1}\,dx \ . \tag{35}$$

In the high temperature limit $T_D \ll T$, $x_D \ll 1$ and $e^x - 1 \approx x$. The integral in Eq. (35) then gives $x_D^3/3$ and hence $U_{\text{vibr}}^{(\text{acoustic})}(T) = 3Nk_BT$; thus for $T \gg T_D$, the heat capacity of the three acoustic branches approaches the value $3Nk_B$ of the Dulong and Petit law.

In the low temperature limit $T \ll T_D$ we can replace $x_D = \infty$, and the integral in Eq. (35) equals $\pi^4/15$ [for a simple and instructive demonstration of the value of this integral see for instance B. D. Sukheeja, Am. J. Phys. **38**, 923 (1970)]. Equation (35) thus gives

$$U_{\text{vibr}}^{(\text{acoustic})}(T) = \frac{3}{5}\pi^4 Nk_B\frac{T^4}{T_D^3} \qquad T \ll T_D \ .$$

Correspondingly, in the low temperature region the heat capacity becomes

$$C_V(T) = \frac{12}{5}\pi^4 Nk_B\frac{T^3}{T_D^3} \qquad T \ll T_D$$

and the correct experimental T^3 behaviour is reproduced.

The Debye model can be refined in several ways. For instance the three acoustic branches could be treated with different sound velocities. In the case of crystals with a basis, one could use the Debye model for the acoustic modes and the Einstein model for the optical modes. We notice that, in the high temperature limit, anharmonic effects are of increasing importance, and corrections to the Dulong and Petit value are likely to be of significance. In metals, besides the vibrational contribution to the internal energy, we have to consider the electronic contribution; the electronic contribution to the heat capacity is proportional to T at any temperature and may become the dominant term at very low temperatures (see Section III-3). We notice finally that the T^3 law depends on the crystal dimensionality. In a two-dimensional crystal, instead of Eq. (33), the density-of-states $D(\omega)$ is proportional to ω and the low temperature lattice heat capacity is characterized by a T^2 power law. Similarly, in an ideal one-dimensional crystal, one would obtain a lattice heat capacity linear in the temperature.

6 Considerations on anharmonic effects and melting of solids

So far we have confined our attention to the harmonic approximation for the lattice vibrations; in this approximation, phonons are elementary excitations of the elastic field, which do not decay and cannot interact. The anharmonic terms, which correspond to cubic, quartic and successive terms in the series expansion of the crystal potential energy, have quite important consequences; for instance, cubic terms make possible three-phonon processes in which one-phonon decays into two phonons or two phonons merge into one. Among the physical effects of anharmonicity, we mention the

thermal expansion of solids, the change of normal mode frequencies with temperature (or other parameters), the thermal resistivity, the broadening of one-phonon peaks in neutron scattering experiments, the solid–liquid transition. It is not our intention to discuss the wealth of problems related to anharmonicity; here we simply provide some intuitive remarks concerning the amplitude of localized motions of the atoms and the Lindemann criterion of melting.

The mean quadratic displacement of a given atom about its equilibrium position is an important quantity, which influences X-ray scattering, cold neutron scattering, Mössbauer effect, and also determines the solid–liquid transition. We wish thus to give an estimate of the mean quadratic displacement of an atom around its equilibrium position as a function of temperature.

For simplicity we consider a three-dimensional crystal with N unit cells and one atom per unit cell. In this case the normal modes consist of three acoustic branches, of frequency $\omega(\mathbf{q},p)$ and polarization vectors $\mathbf{A}(\mathbf{q},p)$ $(p=1,2,3)$. We can expand the displacement $\mathbf{u}_n$ of the atom at $\mathbf{t}_n$ in normal modes; as a straight generalization of Eq. (30a), we have

$$\mathbf{u}_n = \sum_{\mathbf{q}p} \sqrt{\frac{\hbar}{2NM\omega(\mathbf{q},p)}}\, \mathbf{A}(\mathbf{q},p)\, e^{i\mathbf{q}\cdot\mathbf{t}_n} \left[a_{\mathbf{q}p} + a^{\dagger}_{-\mathbf{q}p}\right] . \tag{36}$$

To avoid unessential details, we assume that the three acoustic branches are degenerate, so that $\omega(\mathbf{q},p)$ does not depend on the polarization index p. Furthermore, for any wavevector, the three polarization vectors $\mathbf{A}(\mathbf{q},p)$ form an orthonormal triad, that we intend to orient parallel to some fixed reference frame. Then the component of $\mathbf{u}_n$ along a direction, say z, dropping the now unnecessary polarization index p in Eq. (36) becomes

$$u_{nz} = \sum_{\mathbf{q}} \sqrt{\frac{\hbar}{2NM\omega(\mathbf{q})}}\, e^{i\mathbf{q}\cdot\mathbf{t}_n} \left[a_{\mathbf{q}} + a^{\dagger}_{-\mathbf{q}}\right] .$$

We can now calculate the ensemble average $\langle u_{nz}^2\rangle$ of the quadratic displacement u_{nz}^2. Without loss of generality we take $\mathbf{t}_n = 0$, and use the standard results

$$\langle a^{\dagger}_{\mathbf{q}} a_{\mathbf{q}}\rangle = \frac{1}{\exp(\hbar\omega_{\mathbf{q}}/k_BT)-1} , \qquad \langle a_{\mathbf{q}} a^{\dagger}_{\mathbf{q}}\rangle = \langle a^{\dagger}_{\mathbf{q}} a_{\mathbf{q}}\rangle + 1 ,$$

where $\langle a^{\dagger}_{\mathbf{q}} a_{\mathbf{q}}\rangle$ is the well known Bose population factor (see Appendix A). The average square displacement $\langle u_z^2\rangle$ of each atom thus becomes

$$\boxed{\langle u_z^2\rangle = \sum_{\mathbf{q}} \frac{\hbar}{2NM\omega(\mathbf{q})} \left[\frac{2}{\exp(\hbar\omega(\mathbf{q})/k_BT)-1} + 1\right]} . \tag{37}$$

It is instructive to calculate the average square displacement for the Debye model of the phonon spectrum. We have already seen that the density-of-states for any of

the three branches is given by Eq. (33). Equation (37) thus becomes

$$\langle u_z^2 \rangle = \int_0^{\omega_D} \frac{\hbar}{2NM\omega} \left(\frac{2}{e^{\hbar\omega/k_BT} - 1} + 1 \right) N \frac{3\omega^2}{\omega_D^3} \, d\omega \; .$$

If we introduce the dimensionless variable $x = \hbar\omega/k_BT$ and define $\hbar\omega_D = k_BT_D$, we have

$$\langle u_z^2 \rangle = 3 \frac{\hbar^2 T^2}{M k_B T_D^3} \int_0^{T_D/T} \left(\frac{1}{e^x - 1} + \frac{1}{2} \right) x \, dx \; . \tag{38}$$

The integral can be easily performed in the limits of very high temperatures ($T \gg T_D$) using a series development of the exponential, and of very low temperatures ($T \ll T_D$). We have respectively

$$\langle u_z^2 \rangle = \begin{cases} \dfrac{3}{4} \dfrac{\hbar^2}{M k_B T_D} & \text{for} \quad T \ll T_D \\ \\ 3 \dfrac{\hbar^2 T}{M k_B T_D^2} & \text{for} \quad T \gg T_D \; . \end{cases} \tag{39}$$

From Eq. (39), it is seen that the value of $\langle u_z^2 \rangle$ at zero temperature is only somewhat smaller than the value of $\langle u_z^2 \rangle$ at the Debye temperature; in fact $\langle u_z^2 \rangle_{T=T_D} \approx 4 \langle u_z^2 \rangle_{T=0}$.

We can now establish a simple qualitative criterion for melting. Let r_0 be the mean radius of the unit cell, and consider the ratio

$$f = \frac{\sqrt{\langle u_x^2 \rangle + \langle u_y^2 \rangle + \langle u_z^2 \rangle}}{r_0} = \sqrt{\frac{9\hbar^2 T}{M k_B T_D^2 r_0^2}} \qquad T \gg T_D \; . \tag{40a}$$

When the ratio f reaches a critical value f_c (almost independent from the specific solid in consideration), melting is expected to occur. The melting temperature is thus given by the Lindemann formula

$$T_m = \frac{f_c^2}{9\hbar^2} M k_B T_D^2 r_0^2 \; ; \tag{40b}$$

the critical value f_c turns out to be of the order of 0.2–0.3 in many solids.

Another interesting conclusion can be done on the stability of one-dimensional and two-dimensional crystals. In these cases, the calculation of the mean quadratic displacement in the plane or in the chain (using the appropriate density of phonon states), leads to a divergent value at any temperature. Thus one-dimensional and two-dimensional crystals are unstable in the harmonic approximation; some three-dimensional interaction (whatever small with respect to intralayer or intrachain interaction) is necessary to stabilize low-dimensional structures.

7 Optical phonons and polaritons in polar crystals

7.1 General considerations

In Section 3, we have studied the crystal lattice vibrations by means of the dynamical matrix formalism. The dynamical matrix treatment implicitly assumes that the inter-

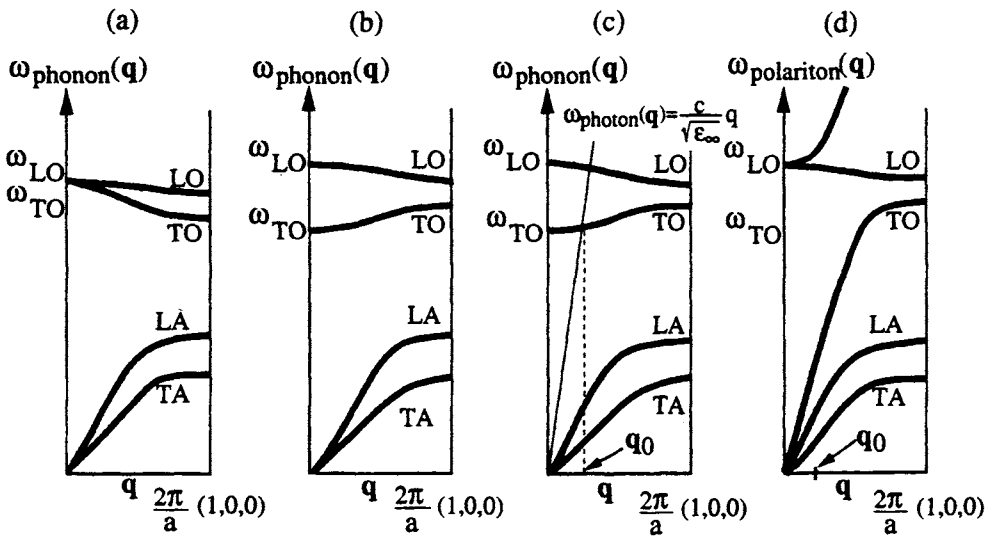

Fig. 9 (a) Schematic behaviour of phonon dispersion curves of a cubic *homopolar* semiconductor (or insulator) with two equal atoms per unit cell, along a high symmetry direction. (b) Schematic behaviour of phonon dispersion curves of a cubic *heteropolar* semiconductor (or insulator) with two different atoms per unit cell, when retardation effects are ignored. (c) Superimposed to the previous phonon dispersion curves, there is now the photon dispersion curve $\omega(\mathbf{q}) = c\,q/\sqrt{\varepsilon_\infty}$, assuming momentarily no coupling between electromagnetic waves and lattice vibrations. We have indicated by $q_0 \approx \sqrt{\varepsilon_\infty}\,\omega_{TO}/c \approx (\sqrt{\varepsilon_\infty}\,v_s/c)(2\pi/a)$ the point at which the photon-like dispersion curve crosses the transverse phonon dispersion curve. In the figure, the slope of the photon dispersion curve (of the order of the velocity of light) and the slope of the acoustic modes (of the order of sound velocity) could not be drawn in scale. (d) Schematic picture of *polariton effects*. Phonons and photons with nearly equal wavevectors and energies interact and determine the polariton dispersion curve. *Polariton effects extend from* $q = 0$ *to approximately* q_0*, which is a fraction of the order of* $v_s/c \approx 10^{-5}$ *of the Brillouin zone dimension* (see Fig. 10 and Fig. 11 for an expanded scale and further details). Notice that polariton effects restore the threefold degeneracy of the state of frequency ω_{LO} at $q = 0$.

atomic interactions are instantaneous. For polar crystals (such as ionic crystals and heteropolar semiconductors), the long-range nature of inter-atomic Coulomb interactions requires a proper account of retardation effects due to the finite velocity of light. The coupling of transverse mechanical waves and electromagnetic waves is particularly important for wavevectors q in the range from $q=0$ to approximately the value q_0, which denotes the crossing point of the dispersion curves of (uncoupled) photons and phonons (see Fig. 9). Before considering a continuous model to describe the optical phonons in polar crystals, we briefly summarize some relevant phenomenological aspects.

As a preliminary to further considerations, let us compare the vibrational curves of homopolar and heteropolar cubic crystals with two atoms per unit cell (see Fig. 6, Fig. 7 and Fig. 8 for specific examples; see also Fig. 9 for a schematic summary of

the important features). From the general discussion of Section 3, we have seen that the dispersion curves of a diatomic crystal consist of three acoustic and three optical branches. In cubic crystals, for vectors $\mathbf{q}$ along high symmetry directions, there are two degenerate transverse acoustic modes (TA) and one longitudinal acoustic mode (LA). Similarly, there are two degenerate transverse optical modes (TO) and one longitudinal optical mode (LO), whose frequencies go to finite values ω_{TO} and ω_{LO} in the long wavelength limit. In nonpolar diatomic cubic crystals, the optical modes for small wavelengths are degenerate, i.e. $\omega_{LO} \equiv \omega_{TO}$ (Fig. 9a). On the contrary, the frequencies ω_{LO} and ω_{TO} of longitudinal and transverse optical phonons are different in polar crystals, in spite of the cubic symmetry (Fig. 9b); this symmetry-breaking effect is due to the long-range nature of the electrostatic forces.

The longitudinal-transverse splitting has implications also on the infrared dielectric properties of polar semiconductors and insulators. These materials are strongly reflecting in the frequency region $\omega_{TO} < \omega < \omega_{LO}$; repeated reflexions can be used to select a band of wavelengths of infrared radiation, which is known as Reststrahlen (residual rays) radiation. Furthermore, the frequencies ω_{LO} and ω_{TO} satisfy the Lyddane–Sachs–Teller relation

$$\boxed{\frac{\omega_{LO}^2}{\omega_{TO}^2} = \frac{\varepsilon_s}{\varepsilon_\infty}}, \tag{41}$$

where ε_s is the static dielectric constant and ε_∞ is the high-frequency dielectric constant. By ε_∞ we mean the infrared dielectric constant at frequencies much higher than a typical phonon frequency (so that ionic displacement contribution can be neglected) and much smaller than any electronic transition frequency; ε_∞ is determined by the electronic contribution to the static dielectric constant. If ω_{LO} and ω_{TO} are significantly different, the same occurs for ε_s and ε_∞ (and vice versa); in some materials (such as ferroelectric ionic crystals), ω_{TO} is anomalously small and ε_s anomalously large.

The electromagnetic coupling between a radiation field and transverse optical phonons leads to the concept of new quasiparticles, known as *polaritons*; photons and transverse phonons strongly interact near the crossing of the corresponding dispersion curves, which are modified into polariton dispersion curves (see Fig. 9c and Fig. 9d). We pass now to interpret the phenomenological properties of polar crystals mentioned above, with a suitable continuous model.

7.2 Lattice vibrations in polar crystals and polaritons

The continuous approximation for optical vibrational modes in isotropic materials

We can establish a reasonable simple model for polaritons, combining a continuous approximation for the description of the mechanical waves of the optical modes and the Maxwell equations for the description of the electromagnetic waves [J. J. Hopfield and D. G. Thomas, Phys. Rev. **132**, 563 (1963)]. We confine our attention here to polar cubic crystals with two atoms (cation and anion) in the unit cell, of effective

charge $\pm e^*$, mass M_1 and M_2 (and reduced mass M^*). In optical vibrational modes, cations and anions move against each other, so we can discuss the motion of the ions in the unit cell by the relative displacement variable $\mathbf{w}$. In analogy with Eq. (19), we expect for isotropic cubic crystals that the relative displacement variable $\mathbf{w}$ obeys the equation of motion

$$\ddot{\mathbf{w}} = -\omega_0^2 \mathbf{w} + \frac{e^*}{M^*}\mathbf{E} \,. \tag{42}$$

Notice that in the case the effective charge e^* vanishes, the three optical modes become degenerate, with frequency $\omega_{TO} = \omega_{LO} = \omega_0$, and are dispersionless. The continuous model, summarized by Eq. (42), is rather simplified, but it has the merit to allow analytic elaborations and to provide guidelines for more complicated situations. Among the limitations of the model, we notice that the local electric field acting on the site effective charge and the average electric field (due to any internal or external sources) are supposed to coincide; local field effects are introduced in Section 7.3.

In order to estimate semi-empirically the quantity e^*/M^*, consider Eq. (42) in the presence of a static electric field $\mathbf{E}_s$; the static ionic displacement is given by $\mathbf{w}_s = (e^*/\omega_0^2 M^*)\mathbf{E}_s$. The average ionic polarization of a crystal, of volume V and N unit cells, is $\mathbf{P}_{\text{ion,s}} = (N/V)e^*\mathbf{w}_s = (N/V)(e^{*2}/\omega_0^2 M^*)\mathbf{E}_s$. The static dielectric constant ε_s and the high-frequency dielectric constant ε_∞ are related by the expression

$$\varepsilon_s = \varepsilon_\infty + 4\pi \frac{P_{\text{ion,s}}}{E_s} = \varepsilon_\infty + \frac{4\pi (N/V) e^{*^2}}{\omega_0^2 M^*} \,.$$

Using the above equation, we can re-write Eq. (42) in the form

$$\ddot{\mathbf{w}} = -\omega_0^2 \mathbf{w} + \omega_0^2 \frac{\varepsilon_s - \varepsilon_\infty}{4\pi (N/V) e^*}\mathbf{E} \,. \tag{43}$$

The ionic contribution to the polarization (dipole per unit volume) of the specimen is given by

$$\mathbf{P}_{\text{ion}} = \frac{N}{V} e^* \mathbf{w} \,.$$

Multiplying both members of Eq. (43) by $(N/V)e^*$ we obtain

$$\boxed{\ddot{\mathbf{P}}_{\text{ion}} = -\omega_0^2 \mathbf{P}_{\text{ion}} + \omega_0^2 \frac{\varepsilon_s - \varepsilon_\infty}{4\pi}\mathbf{E}} \,. \tag{44}$$

Equation (44) is the very useful "constitutive" equation of polar crystals; it couples the electric polarization, produced by the vibrating lattice of ions, to the electric field in the crystal; the phenomenological coupling constant is given by $\omega_0^2(\varepsilon_s - \varepsilon_\infty)/4\pi$.

We consider first the propagation in the medium of *longitudinal optical vibrations*, in which case the polarization field and the electric field are also expected to be of longitudinal type with the form

$$\mathbf{P}_{\text{ion}}(\mathbf{r}, t) = \mathbf{P}_0 \, e^{i(\mathbf{q}\cdot\mathbf{r} - \omega t)} \quad \text{with} \quad \mathbf{P}_0 \| \mathbf{q} \tag{45a}$$

$$\mathbf{E}(\mathbf{r}, t) = \mathbf{E}_0 \, e^{i(\mathbf{q}\cdot\mathbf{r} - \omega t)} \quad \text{with} \quad \mathbf{E}_0 \| \mathbf{q} \,. \tag{45b}$$

We can easily show that for longitudinal fields we have

$$\boxed{\mathbf{E}_0 = -\frac{4\pi}{\varepsilon_\infty}\mathbf{P}_0} \qquad \mathbf{E}_0 \| \mathbf{P}_0 \| \mathbf{q} \,. \tag{45c}$$

In fact the microscopic charge density accompanying the polarization field (45a) is given by $\rho_{\text{micr}} = -\text{div}\,\mathbf{P}_{\text{ion}} = -iqP_0 \exp(i\mathbf{q}\cdot\mathbf{r} - i\omega t)$; the value $\mathbf{E}_0$ is determined so that $\text{div}\,\mathbf{E} = iqE_0 \exp(i\mathbf{q}\cdot\mathbf{r} - i\omega t) \equiv 4\pi\rho_{\text{micr}}/\varepsilon_\infty$. Also notice that the curl of the longitudinal fields (45) vanish identically.

Inserting Eqs. (45) into Eq. (44), it is found that the frequency ω for the longitudinal waves satisfies

$$-\omega^2 = -\omega_0^2 - \omega_0^2 \frac{\varepsilon_s - \varepsilon_\infty}{\varepsilon_\infty} \equiv -\omega_0^2 \frac{\varepsilon_s}{\varepsilon_\infty} \,.$$

Thus the longitudinal waves are characterized by the dispersionless relation

$$\omega^2 = \omega_0^2 \frac{\varepsilon_s}{\varepsilon_\infty} \equiv \omega_{LO}^2 \,. \tag{46}$$

The effect of the long-range Coulomb field on the longitudinal optical vibrations does not introduce any dispersion; it however does increase the "restoring forces" and does increase the oscillation frequency from ω_0 (the value neglecting long-range contributions) to ω_{LO}.

We consider now the propagation in the medium of *transverse optical vibrations*, in which case the polarization field and the electric field are of transverse type, with the form

$$\mathbf{P}_{\text{ion}}(\mathbf{r}, t) = \mathbf{P}_0 \, e^{i(\mathbf{q}\cdot\mathbf{r} - \omega t)} \qquad \text{with} \quad \mathbf{P}_0 \perp \mathbf{q} \tag{47a}$$

$$\mathbf{E}(\mathbf{r}, t) = \mathbf{E}_0 \, e^{i(\mathbf{q}\cdot\mathbf{r} - \omega t)} \qquad \text{with} \quad \mathbf{E}_0 \perp \mathbf{q} \,. \tag{47b}$$

It is shown below that for transverse fields we have

$$\boxed{\mathbf{E}_0 = \frac{4\pi\omega^2}{c^2q^2 - \varepsilon_\infty\omega^2}\mathbf{P}_0} \qquad \mathbf{E}_0 \| \mathbf{P}_0 \perp \mathbf{q} \,. \tag{47c}$$

From Eq. (47c) it is seen that the ratio E_0/P_0 for transverse fields depends both on q and ω, contrary to the situation for longitudinal fields expressed by Eq. (45c); also notice that for $q \to 0$ and finite ω, Eq. (47c) coincide with Eq. (45c), and the transverse and longitudinal polaritons become thus degenerate.

It is worthwhile to remark that the divergence of the transverse fields vanishes identically (in particular $\rho_{\text{micr}} = -\text{div}\,\mathbf{P}_{\text{ion}} \equiv 0$ means that no microscopic charge is accompanying the polarization wave, and thus also $\text{div}\,\mathbf{E} \equiv 0$). For transverse fields $\text{curl}\,\mathbf{E} \neq 0$; before considering the correct treatment of $\text{curl}\,\mathbf{E}$ with the Maxwell equations, we examine the so called *electrostatic limit* (also called the $c \to \infty$ limit, or instantaneous interaction limit, or omission of retardation effects), which just consists in taking $\text{curl}\,\mathbf{E} = 0$. Since also $\text{div}\,\mathbf{E} = 0$, we conclude that the electric field accompanying a transverse optical vibration vanishes; the frequency of the optical transverse modes would be unchanged with respect to ω_0 in the electrostatic approximation.

For the correct determination of curl $\mathbf{E}$, we have to resort to the appropriate Maxwell equations

$$\operatorname{curl}\mathbf{E} = -\frac{1}{c}\frac{\partial \mathbf{B}}{\partial t} \tag{48a}$$

$$\operatorname{curl}\mathbf{H} = \frac{1}{c}\frac{\partial \mathbf{D}}{\partial t} = \frac{\varepsilon_\infty}{c}\frac{\partial \mathbf{E}}{\partial t} + \frac{4\pi}{c}\frac{\partial \mathbf{P}_{\text{ion}}}{\partial t} . \tag{48b}$$

From the curl of both members of Eq. (48a), and using Eq. (48b) (in non-magnetic materials $\mathbf{B} = \mathbf{H}$), we have

$$\operatorname{curl}\operatorname{curl}\mathbf{E} = -\frac{\varepsilon_\infty}{c^2}\ddot{\mathbf{E}} - \frac{4\pi}{c^2}\ddot{\mathbf{P}}_{\text{ion}} .$$

For transverse fields $\operatorname{div}\mathbf{E} = 0$; using the vectorial identity $\operatorname{curl}\operatorname{curl} = \operatorname{grad}\operatorname{div} - \nabla^2$, it follows

$$-\nabla^2\mathbf{E} = -\frac{\varepsilon_\infty}{c^2}\ddot{\mathbf{E}} - \frac{4\pi}{c^2}\ddot{\mathbf{P}}_{\text{ion}} ; \tag{49}$$

it is then seen by inspection that Eq. (47a) and Eq. (47b) imply Eq. (47c).

We insert now Eqs. (47) into the constitutive Eq. (44) and obtain the compatibility condition

$$\varepsilon_\infty\omega^4 - (\omega_0^2\varepsilon_s + c^2q^2)\omega^2 + \omega_0^2c^2q^2 = 0 . \tag{50}$$

We can solve for ω^2 and obtain the dispersion relation for polaritons

$$\omega^2 = \frac{1}{2\varepsilon_\infty}\left[\omega_0^2\varepsilon_s + c^2q^2 \pm \sqrt{(\omega_0^2\varepsilon_s + c^2q^2)^2 - 4\omega_0^2c^2q^2\varepsilon_\infty}\right] . \tag{51}$$

The dispersion curves for polaritons, given by Eq. (51), are schematically shown in Fig. 10.

It is interesting to examine the lower and upper polariton branches in the limit of $q < q_0$ and $q > q_0$, where q_0 is the point for which $(c/\sqrt{\varepsilon_\infty})\,q_0 \equiv \omega_{TO}$. For $q \gg q_0$, the two solutions of Eq. (51), and the corresponding amplitudes $\mathbf{E}_0$ and $\mathbf{P}_0$ given by Eq. (47c) are

$$\omega^2 = \omega_0^2 = \omega_{T0}^2 \qquad \mathbf{E}_0 = 0 \qquad \mathbf{P}_0 \neq 0$$

and

$$\omega^2 = \frac{c^2}{\varepsilon_\infty}q^2 \qquad \mathbf{P}_0 = 0 \qquad \mathbf{E}_0 \neq 0 ;$$

thus for $q \gg q_0$ the lower branch is a pure mechanical wave (with $\mathbf{E}_0 = 0$) and the upper branch is a pure electromagnetic wave (with $\mathbf{P}_0 = 0$).

For $q \ll q_0$, the two solutions of Eq. (51), and the corresponding amplitudes $\mathbf{E}_0$ and $\mathbf{P}_0$ given by Eq. (47c) are

$$\omega^2 = \omega_0^2\frac{\varepsilon_s}{\varepsilon_\infty} = \omega_{LO}^2 \qquad \mathbf{E}_0 = -\frac{4\pi}{\varepsilon_\infty}\mathbf{P}_0$$

and

$$\omega^2 = \frac{c^2}{\varepsilon_s}q^2 \qquad \mathbf{P}_0 = \frac{\varepsilon_s - \varepsilon_\infty}{4\pi}\mathbf{E}_0 .$$

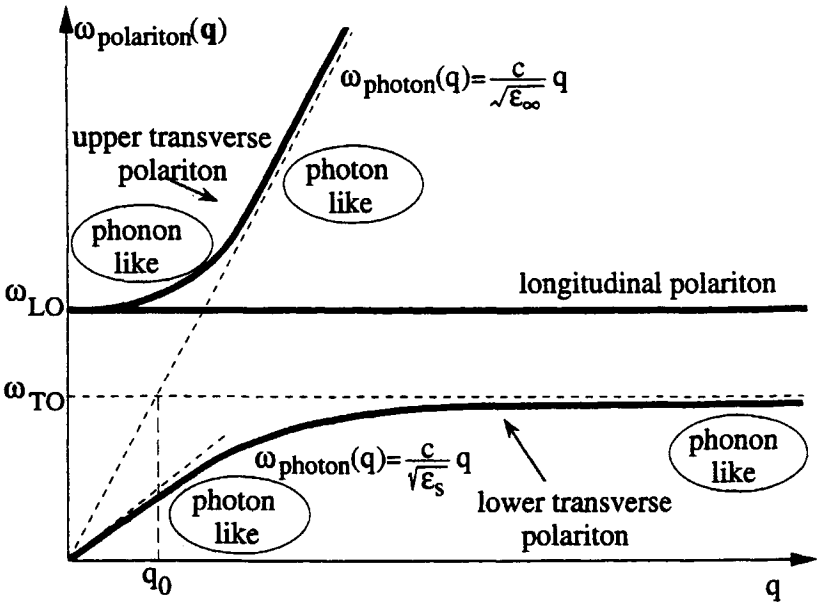

Fig. 10 Schematic description of polaritons. The dispersion curves of uncoupled transverse phonons and photons are shown by dashed lines; q_0 is the crossing point $q_0 = \omega_{TO}/(c/\sqrt{\varepsilon_\infty})$; dispersion curves of the longitudinal phonon and transverse polaritons are shown by solid lines. In the lower polariton branch, the character of the dispersion curve changes from photon-like for $q < q_0$ to phonon-like for $q > q_0$; in the upper branch, the character changes from phonon-like to photon-like as q increases.

Thus for q smaller or near q_0 the polariton modes have the character of coupled mechanical–electromagnetic waves, with $\mathbf{E}_0$ and $\mathbf{P}_0$ *simultaneously* different from zero. Notice in particular that for $\omega = \omega_{LO}$ we have $\mathbf{E}_0 = -(4\pi/\varepsilon_\infty)\mathbf{P}_0$ both for transverse and longitudinal waves (see Eq. 45c); thus the degeneracy of transverse and longitudinal modes is restored at $\mathbf{q} = 0$.

As an illustrative example of the concepts developed so far, we report in Fig. 11 the polariton dispersion curves in GaP. The dispersion curves for optical phonons of long wavelength, in the absence of coupling to photons, are horizontal straight lines; transverse optical phonons and photons with nearly the same energy and wavevector are strongly coupled by the phonon–photon interaction and lead to the polariton dispersion curves.

We have seen that transverse optical phonons and photons with nearly the same energy and wavevector are strongly coupled; we notice that quite similar coupling effects occur also for photons and transverse excitons (exciton states have been studied in Section VII-1). The mixed exciton–photon states are called exciton–polaritons and their dispersion curves have a behaviour qualitatively similar to the polariton curves so far discussed [see for instance L. C. Andreani in "Confined Electrons and Photons: New Physics and Devices" edited by E. Burnstein and C. Weisbuch, Plenum Press

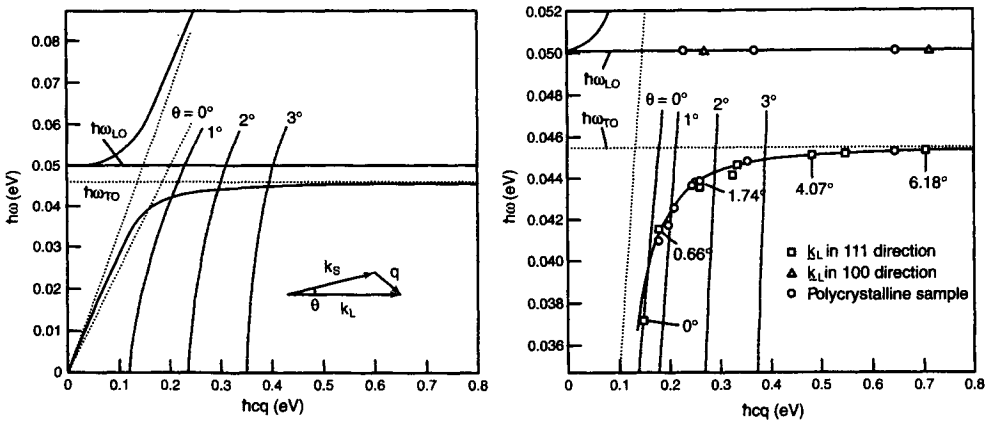

Fig. 11 Polariton dispersion curves in GaP. In Fig. 11a the vector diagram of Raman spectroscopy measurements is also indicated; $\mathbf{k}_L$, $\mathbf{k}_S$ and $\mathbf{q}$ are the wavevectors of the incident laser photon, scattered Stokes photon, and polariton; θ is the scattering angle. Values of energies and wavevectors which are kinematically possible at angle θ are shown by long-dashed lines. In Fig. 11b the plot of the observed energies and wavectors of polaritons and LO phonons are given. The figures are taken from C. H. Henry and J. J. Hopfield, Phys. Rev. Lett. **15**, 964 (1965); copyright 1965 by the American Physical Society.

1995, p.57, and references quoted therein]. An example of dispersion curves of exciton–polaritons in CuCl is reported in Fig. 12.

Infrared dielectric properties of polar crystals

We can now discuss the infrared dielectric properties of polar crystals exploiting the "constitutive" equation (44), that couples the ionic polarization to the electric field in the medium. We consider the response of the system to a time-dependent driving electric field, periodic in space and time, of the form

$$\mathbf{E}(\mathbf{r},t) = \mathbf{E}_0\, e^{i(\mathbf{q}\cdot\mathbf{r}-\omega t)} e^{\eta t}\ ; \tag{52a}$$

the electric field is turned on adiabatically from $t = -\infty$, and this is achieved through the exponential factor $\exp(\eta t)$ with $\eta \to 0^+$. By analogy to Eq. (52a), we assume for $\mathbf{P}_{\text{ion}}$ the expression

$$\mathbf{P}_{\text{ion}}(\mathbf{r},t) = \mathbf{P}_0\, e^{i(\mathbf{q}\cdot\mathbf{r}-\omega t)} e^{\eta t}\ . \tag{52b}$$

Replacing Eqs. (52) into Eq. (44), one obtains

$$\mathbf{P}_0 = \frac{\omega_0^2}{\omega_0^2 - (\omega + i\eta)^2} \frac{\varepsilon_s - \varepsilon_\infty}{4\pi}\, \mathbf{E}_0 \tag{53}$$

(for the present model under consideration, it is irrelevant whether $\mathbf{E}_0$ and $\mathbf{P}_0$ are parallel or orthogonal to the vector $\mathbf{q}$).

The dielectric function is given by $\varepsilon(\omega) = \varepsilon_\infty + 4\pi P_0/E_0$, where as before ε_∞ denotes the dielectric constant due to the electronic polarizability (at frequencies well

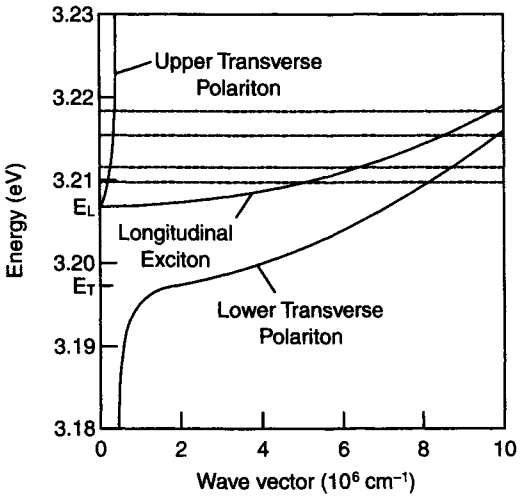

Fig. 12 Dispersion curves of the transverse exciton–polaritons of CuCl in the anomalous dispersive region. The dashed lines refer to the laser energies used to study luminescence line shape due the decay from bound pairs of excitons [from J. K. Pribram, G. L. Koos, F. Bassani and J. P. Wolfe, Phys. Rev. **B28**, 1048 (1983); copyright 1983 by the American Physical Society].

below any electronic transition resonance). Using Eq. (53), we obtain for the dielectric function of the polar crystal

$$\boxed{\varepsilon(\omega) = \varepsilon_\infty + \frac{\omega_0^2}{\omega_0^2 - \omega^2 - i\eta\omega}(\varepsilon_s - \varepsilon_\infty)} \tag{54}$$

(where 2η has been relabelled as η). The real and imaginary parts of the dielectric function are schematically indicated in Fig. 13.

In the limit of $\eta \to 0^+$ the real and imaginary parts of Eq. (54) become

$$\varepsilon_1(\omega) = \varepsilon_\infty + \frac{\omega_0^2}{\omega_0^2 - \omega^2}(\varepsilon_s - \varepsilon_\infty) = \frac{\varepsilon_s \omega_0^2 - \varepsilon_\infty \omega^2}{\omega_0^2 - \omega^2} \tag{55a}$$

and

$$\varepsilon_2(\omega) = \frac{\pi\omega_0(\varepsilon_s - \varepsilon_\infty)}{2}\left[\delta(\omega - \omega_0) - \delta(\omega + \omega_0)\right] . \tag{55b}$$

At positive frequencies, $\varepsilon_1(\omega)$ exhibits a pole for $\omega = \omega_0 = \omega_{TO}$ (transverse phonon frequency) and has a zero for $\omega = \omega_0\sqrt{\varepsilon_s/\varepsilon_\infty} = \omega_{LO}$ (longitudinal phonon frequency); the values ω_{TO} and ω_{LO} satisfy the Lyddane–Sachs–Teller relation (41).

The dielectric function $\varepsilon_1(\omega)$ is negative for $\omega_{TO} < \omega < \omega_{LO}$. In this region the reflectivity equals one, and the electromagnetic propagation in the crystal is forbidden. Outside the interval $[\omega_{TO}, \omega_{LO}]$ the dielectric function $\varepsilon_1(\omega)$ is positive and $\varepsilon_2(\omega)$ vanishes (when $\eta \to 0^+$); in this region, the dispersion relations for electromagnetic

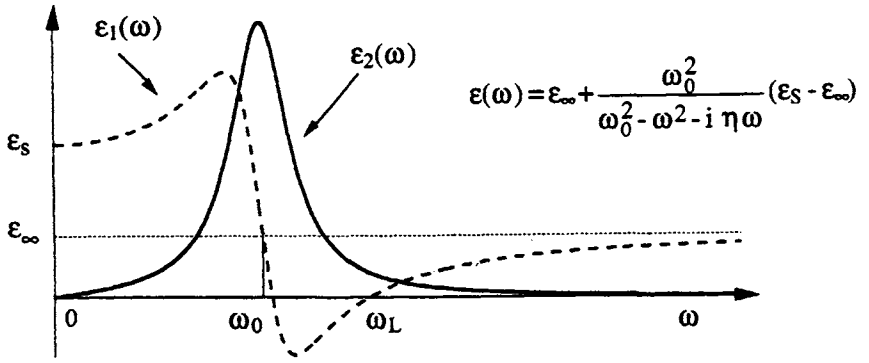

Fig. 13 Schematic behaviour of the real and imaginary part of the dielectric function $\varepsilon(\omega)$ of a polar crystal in the infrared region. Since $\varepsilon_1(\omega)$ and $\varepsilon_2(\omega)$ are even and odd functions of ω, respectively, only the part $\omega > 0$ is indicated. For $\eta \to 0^+$, the real part $\varepsilon_1(\omega)$ presents a pole at $\omega = \omega_0$, while the imaginary part $\varepsilon_2(\omega)$ presents a δ-like singularity at $\omega = \omega_0$.

waves propagating in a medium are determined by the requirement

$$\omega = \frac{c}{\sqrt{\varepsilon_1(\omega)}} q \tag{56a}$$

(see also the discussion at the end of Section XI-1). We have $\omega^2 \varepsilon_1(\omega) = c^2 q^2$; using for $\varepsilon_1(\omega)$ the expression (55a), we obtain

$$\omega^2 \frac{\varepsilon_s \omega_0^2 - \varepsilon_\infty \omega^2}{\omega_0^2 - \omega^2} = c^2 q^2 \,. \tag{56b}$$

It can be immediately seen that Eq. (56b) coincides exactly with Eq. (50), and defines thus the dispersion curves of the polaritons in the crystal.

7.3 Local field effects on polaritons

The internal field according to Lorentz

In the discussion of Section 7.2 we have assumed that the macroscopically averaged electric field $\mathbf{E}$ and the local field $\mathbf{E}_{\text{loc}}$ are the same. In solids, however, there can be significant differences betweeen the two fields, and a central (and not easy) problem in the theory of dielectrics is the calculation of the electric field at the position of a given atom or molecule. Without entering in all the subtleties of this problem, we here briefly discuss the internal field according to Lorentz.

Consider an isotropic dielectric crystal with the shape of a bar, very long in the z-direction (see Fig. 14). Imagine that microscopic electric dipoles are set up at the lattice points so to give rise to a uniform polarization $\mathbf{P}$ in the z direction. We notice that since $\mathbf{P}$ is uniform, we have $\rho_{\text{micr}} = -\text{div}\,\mathbf{P} = 0$ and no volume microscopic charge density is accompanying the polarization. We also notice that the geometry of the (thin and very long) bar is chosen so that $\mathbf{P}$ is parallel to the surface of the sample;

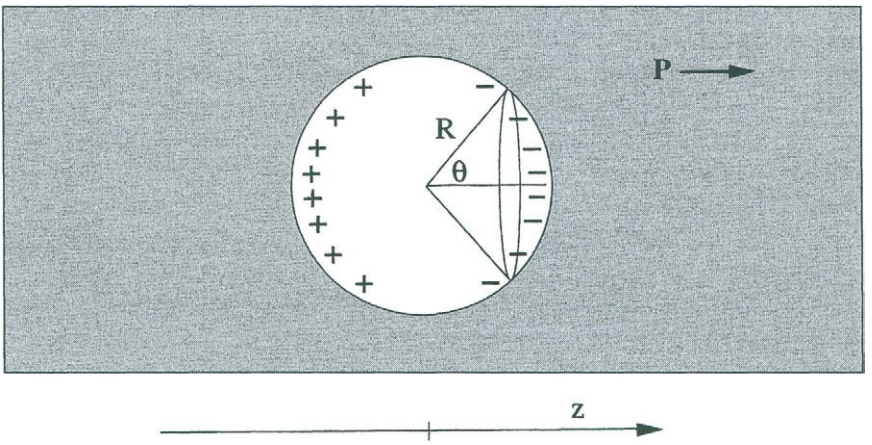

Fig. 14 Schematic representation of the Lorentz cavity for the calculation of the local electric field. The sample (with the ideal shape of a thin and infinitely long bar) is supposed to be uniformly polarized with **P** parallel to the surface of the sample.

thus no discontinuity of the normal component of **P** occurs at the surfaces, and no microscopic surface charge density occurs either. Because of the absence of any internal and external charges, we have $\operatorname{div}\mathbf{E} = 0$; in stationary situations also $\operatorname{curl}\mathbf{E} = 0$ and the electric field is thus zero.

Although the uniformly polarized specimen in the geometry of Fig. 14 is in a *null electric field*, it is easily realized that the *local electric field acting on the microscopic dipoles*, which are the origin of the macroscopic polarization field **P**, is in general different from zero. For simplicity, we confine our attention to the extreme tight-binding limit, in which the crystal can be viewed as a collection of microscopic electric dipoles, well localized around the lattice sites; in this case, the local field can be obtained with the following arguments.

Imagine we carve a small spherical region around the site at which the local field is to be evaluated. The medium contained in this region is considered as a discretized collection of dipoles and we determine the electric field at the center of the cavity by summing up the electric fields generated by every dipole (except the one at the origin); when certain conditions of symmetry are fulfilled, the sum may vanish. For simplicity, we focus our attention on structures with sufficiently high local symmetry (some cubic structures, for instance), so that the electric field generated by the point-like dipoles within the cavity vanishes at its center.

The uniformly polarized medium outside the Lorentz cavity is dealt with in the continuum approximation (Fig. 14). The contribution due to the dipoles outside the ideal cavity, of radius R, can be obtained noticing that the discontinuity of the component of **P** normal to the surface implies a microscopic density of surface polarization charge given by

$$\sigma_p = P_n = -P\cos\theta\ .$$

The electric field in the z direction at the center of the cavity due to the polarization charges at the cavity surface is

$$E_0 = \int_0^{\pi} (-P\cos\theta)\cdot R\,d\theta\cdot 2\pi R\sin\theta\cdot\frac{-1}{R^2}\cos\theta = \frac{4\pi}{3}P\ . \tag{57}$$

From Eq. (57), we see that in (above specified) isotropic materials in null electric field, the local field is $(4\pi/3)\mathbf{P}$. If the electric field $\mathbf{E}$ applied to the material is different from zero, we have that the local field acting on the dipoles is the sum of $\mathbf{E}$ and $(4\pi/3)\mathbf{P}$. In summary, in the Lorentz model, the relationship between local field, average macroscopic field and electric polarization is given by

$$\mathbf{E}_{\text{loc}} = \mathbf{E} + \frac{4\pi}{3}\mathbf{P}\ . \tag{58a}$$

The above expression has several limitations. These may be due to the overlapping of electronic clouds, or dipolar fields far from homogeneity. At times the Lorentz field is better approximated by the generalized form

$$\mathbf{E}_{\text{loc}} = \mathbf{E} + \gamma\frac{4\pi}{3}\mathbf{P}\ , \tag{58b}$$

where γ is a semi-empirical parameter. The case $\gamma = 0$ indicates no distinction between local and average field (this is the case of free electrons or essentially spread out wavefunctions), while $\gamma = 1$ is the case of strong localized dipoles in highly symmetric crystals. In even more refined models, γ may be different for different sublattices.

Internal field, polarizability and dielectric constant of materials

Consider a system that can be visualized as constituted by N atoms (or molecules) in the volume V, and suppose for simplicity that the interaction between different atoms (or molecules) can be neglected. We wish to express the dielectric constant ε of the material in terms of the polarizability α of the composing units.

In the presence of an applied field $\mathbf{E}$, the average polarization due to induced dipoles of polarizability α is

$$\mathbf{P} = \frac{N}{V}\alpha\,\mathbf{E}_{\text{loc}} = \frac{N}{V}\alpha(\mathbf{E} + \gamma\frac{4\pi}{3}\mathbf{P})\ .$$

Hence

$$\mathbf{P} = \frac{(N/V)\alpha}{1 - \gamma(4\pi/3)(N/V)\alpha}\mathbf{E}\ . \tag{59}$$

It is interesting a brief discussion of Eq. (59). In the case the local field and the macroscopic field are the same ($\gamma = 0$), we have $\mathbf{P} = (N/V)\alpha\mathbf{E}$; the polarization $\mathbf{P}$ is thus finite for any finite polarizability. In the case the local field and the macroscopic field are different ($\gamma \neq 0$), the polarization tends to diverge if $\gamma(4\pi/3)(N/V)\alpha \to 1$; this condition is known as "polarization catastrophe". For ordinary dielectrics, the denominator in Eq. (59) is safely far from vanishing condition. For very special crystals, candidate to become ferroelectric, the polarization catastrophe considerations are basic for understanding physical and structural properties near phase transition. Notice that

the polarization catastrophe concept is inherent to the local field theory ($\gamma \neq 0$) and is essentially a cooperative effect.

From Eq. (59), we obtain for the dielectric constant ($\varepsilon = 1 + 4\pi P/E$) the expression

$$\boxed{\varepsilon = 1 + \frac{4\pi(N/V)\alpha}{1 - \gamma(4\pi/3)(N/V)\alpha}} \,. \tag{60}$$

Equation (60) expresses the dielectric constant in terms of the polarizability α of the composing units and of the parameter γ, which characterizes the local field. In the specific case $\gamma = 1$ (Lorentz field), Eq. (60) becomes

$$\varepsilon = 1 + \frac{4\pi(N/V)\alpha}{1 - (4\pi/3)(N/V)\alpha} \,. \tag{61a}$$

The Lorentz formula (61a) can also be written in the form

$$\frac{\varepsilon - 1}{\varepsilon + 2} = \frac{4\pi}{3}\frac{N}{V}\alpha \,, \tag{61b}$$

which is named Lorentz–Lorenz (or Clausius–Mossotti) relation.

Infrared dielectric function and polaritons in polar crystals in the presence of local field effects

In Section 7.2 the study of polaritons and optical properties of polar crystals in the infrared region has been done starting from the equation of motion (42). In the presence of local field effects we have rather to consider the equation of motion of the type

$$\ddot{\mathbf{w}} = -\omega_0^2 \mathbf{w} + \frac{e^*}{M^*}\mathbf{E}_{\text{loc}} \,. \tag{62}$$

We now study the consequences brought about by the fact that the local electric field and the macroscopic electric field may be different.

Consider Eq. (62) when the electric field and the relative displacement are periodic in space and time with the form

$$\mathbf{E}_{\text{loc}} = \mathbf{E}_0\, e^{i(\mathbf{q}\cdot\mathbf{r}-\omega t)} e^{\eta t} \quad \text{and} \quad \mathbf{w} = \mathbf{w}_0\, e^{i(\mathbf{q}\cdot\mathbf{r}-\omega t)} e^{\eta t} \,;$$

the exponential $\exp(\eta t)$ with $\eta \to 0^+$ has been included, so that the electric field is turned on adiabatically at $t = -\infty$. We obtain

$$-(\omega + i\eta)^2\, \mathbf{w}_0 = -\omega_0^2\, \mathbf{w}_0 + \frac{e^*}{M^*}\mathbf{E}_0 \,.$$

Thus the ionic polarizability becomes

$$\alpha_{\text{ion}}(\omega) \equiv \frac{e^* w_0}{E_0} = \frac{e^{*2}}{M^*}\frac{1}{\omega_0^2 - (\omega + i\eta)^2} = \frac{e^{*2}}{M^*\omega_0^2}\frac{\omega_0^2}{\omega_0^2 - \omega^2 - i\eta\omega}$$

(where 2η has been relabeled as η). The ionic polarizability has a significant frequency dependence in the infrared region.

Let us indicate with α_+ and α_- the electronic polarizabilities of the cation and the

anion of the polar crystal; in the infrared region we can neglect any frequency dependence of electronic polarizabilities. Assuming that electronic and ionic polarizabilities add up, the total polarizability (per unit cell) becomes

$$\alpha_{\text{tot}}(\omega) = \alpha_+ + \alpha_- + \frac{e^{*2}}{M^*\omega_0^2}\,\frac{\omega_0^2}{\omega_0^2 - \omega^2 - i\eta\omega}\,. \tag{63}$$

Inserting Eq. (63) into Eq. (60), we obtain for the dielectric function

$$\varepsilon(\omega) = 1 + \frac{4\pi\dfrac{N}{V}\left[\alpha_+ + \alpha_- + \dfrac{e^{*2}}{M^*\omega_0^2}\,\dfrac{\omega_0^2}{\omega_0^2 - \omega^2 - i\eta\omega}\right]}{1 - \gamma\dfrac{4\pi}{3}\dfrac{N}{V}\left[\alpha_+ + \alpha_- + \dfrac{e^{*2}}{M^*\omega_0^2}\,\dfrac{\omega_0^2}{\omega_0^2 - \omega^2 - i\eta\omega}\right]}\,. \tag{64}$$

It is convenient to introduce the quantities A_{el} and A_{ion} defined as

$$A_{\text{el}} = \frac{4\pi}{3}\frac{N}{V}(\alpha_+ + \alpha_-) \quad \text{and} \quad A_{\text{ion}} = \frac{4\pi}{3}\frac{N}{V}\frac{e^{*2}}{M^*\omega_0^2}\,.$$

We can re-write Eq. (64) in the form

$$\varepsilon(\omega) = 1 + \frac{3(A_{\text{el}} + A_{\text{ion}})\omega_0^2 - 3A_{\text{el}}(\omega^2 + i\eta\omega)}{(1 - \gamma A_{\text{el}} - \gamma A_{\text{ion}})\omega_0^2 - (1 - \gamma A_{\text{el}})(\omega^2 + i\eta\omega)}\,. \tag{65}$$

With an eye to the denominator of Eq. (65) we define the "renormalized transverse frequency" ω_{TO} as

$$\omega_{TO}^2 = \omega_0^2\frac{1 - \gamma A_{\text{el}} - \gamma A_{\text{ion}}}{1 - \gamma A_{\text{el}}} \tag{66}$$

(notice that in the case local field effects are negligible $\gamma = 0$ and $\omega_{TO} = \omega_0$). From Eq. (65) we obtain

$$\varepsilon(\omega) = 1 + \frac{3(A_{\text{el}} + A_{\text{ion}})\omega_0^2 - 3A_{\text{el}}(\omega^2 + i\eta\omega)}{1 - \gamma A_{\text{el}}}\,\frac{1}{\omega_{TO}^2 - (\omega^2 + i\eta\omega)}\,. \tag{67}$$

The above expression, in the limiting case of static and high-frequency regions, takes the values

$$\varepsilon_{\text{s}} = 1 + \frac{3(A_{\text{el}} + A_{\text{ion}})\omega_0^2}{(1 - \gamma A_{\text{el}})\omega_{TO}^2} \quad \text{and} \quad \varepsilon_\infty = 1 + \frac{3A_{\text{el}}}{1 - \gamma A_{\text{el}}}\,.$$

Eq. (67) thus becomes

$$\varepsilon(\omega) = 1 + \frac{(\varepsilon_s - 1)\omega_{TO}^2 - (\varepsilon_\infty - 1)(\omega^2 + i\eta\omega)}{\omega_{TO}^2 - (\omega^2 + i\eta\omega)} \equiv \varepsilon_\infty + \frac{\omega_{TO}^2}{\omega_{TO}^2 - \omega^2 - i\eta\omega}(\varepsilon_{\text{s}} - \varepsilon_\infty)\,. \tag{68}$$

Comparison of Eq. (68) with Eq. (54) is self-explanatory; we see that local field effects do not change the form of $\varepsilon(\omega)$, except for the "renormalization" of the transverse and longitudinal frequencies ω_{TO} and ω_{LO}. In particular the transverse frequency (66) decreases with respect to the short-range value ω_0 as an effect of long-range Coulomb interaction and tends to become *soft*. In any case the renormalized transverse and longitudinal frequencies are still related by the Lyddane–Sachs–Teller relation, as this depends on the analytic structure of the response function, rather than on the details

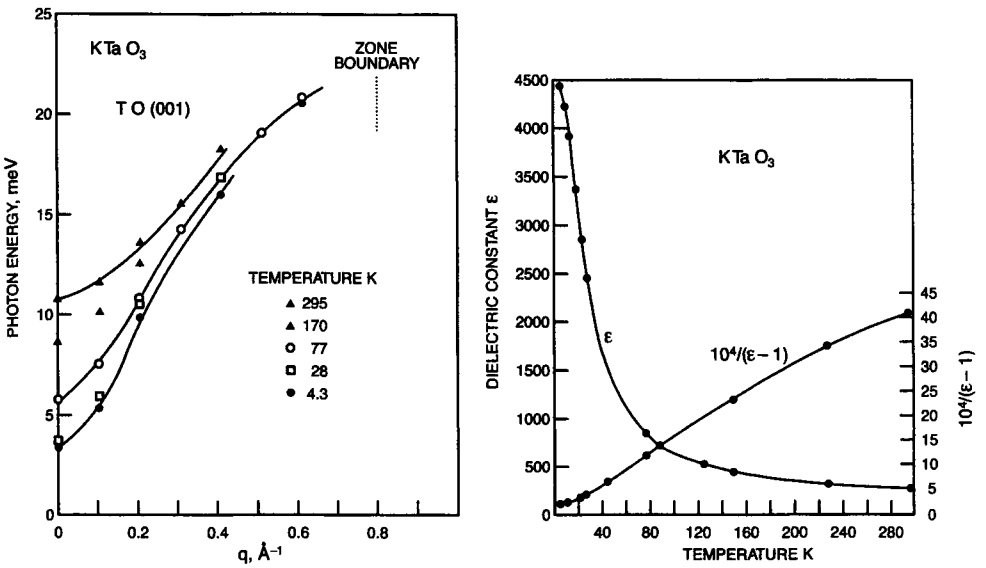

Fig. 15 (a) Temperature dependence of the soft transverse-optical branch in $KTaO_3$ [from G. Shirane, R. Nathans and V. J. Minkiewicz, Phys. Rev. **157**, 396 (1967); copyright 1967 by the American Physical Society]. (b) Dielectric constant and reciprocal susceptibility of $KTaO_3$ as a function of temperature [from S. H. Wemple, Phys. Rev. **137**, A1575 (1965); copyright 1965 by the American Physical Society].

of the orienting fields. We do not have to discuss again the polariton dispersion curves, as the treatment can be performed following step-by-step the previous section, once transverse and longitudinal frequencies are renormalized (as specified by Eq. (66)).

An interesting implication of the local field theory is the possible occurrence of *soft phonon modes*. From Eq. (66) we see that ω_{TO} is reduced with respect to ω_0, since the long-range Coulomb interaction tends to counteract the short-range restoring forces. In the case, due to some mechanism, the frequency ω_{TO} tends to zero, from the Lyddane–Sachs–Teller relation we expect that ε_s tends to infinity. Thus a polar crystal, which exhibits a transverse optical branch with a low frequency mode ω_{TO}, is candidate to develop an extraordinary large polarization. Eventually the crystal might undergo a phase transition and acquire a spontaneous polarization, even in the absence of external fields. Neutron measurements and far infrared optical measurements well support the role of a soft transverse branch in some perovskite ionic crystals.

As an example, we consider the case of perovskite potassium tantalite, and we report in Fig. 15 the temperature dependence of the soft transverse-optical branch (studied by inelastic neutron scattering techniques), as well as the dielectric constant measurements. From Fig. 15 it can be seen that the phonon energy of the soft mode at $q = 0$ is 10.7 meV at 295 K, and decreases to 3.1 meV at 4 K; correspondingly the dielectric constant passes from the value $\varepsilon = 243$ at 295 K to very large values (exceeding several thousands) at low temperatures.

Appendix A. Quantum theory of the linear harmonic oscillator

Creation and annihilation operators

We summarize here some results of the quantum theory of the linear harmonic oscillator, that are preliminary and useful for the discussion of lattice vibrations of crystals.

Consider a one-dimensional harmonic oscillator, of angular frequency ω, described by the Hamiltonian

$$H = \frac{1}{2M} p_x^2 + \frac{1}{2} M\omega^2 x^2 \ . \tag{A1}$$

The lowering (or annihilation) operator and the raising (or creation) operator are defined by the following linear transformations of the observables x and p_x

$$\begin{aligned} a &= \sqrt{\frac{M\omega}{2\hbar}}\, x + i\sqrt{\frac{1}{2\hbar M\omega}}\, p_x \\ a^\dagger &= \sqrt{\frac{M\omega}{2\hbar}}\, x - i\sqrt{\frac{1}{2\hbar M\omega}}\, p_x \ . \end{aligned} \tag{A2}$$

The operators a and $a^\dagger$ satisfy the commutation rule

$$[a, a^\dagger] = 1 \ . \tag{A3}$$

In terms of a and $a^\dagger$, the Hamiltonian (A1) takes the form

$$H = \hbar\omega(a^\dagger a + \frac{1}{2}) \ , \tag{A4}$$

as can be easily verified inserting expression (A2) into Eq. (A4).

In order to work out eigenvalues and eigenfunctions of the Hamiltonian (A4), we note a few relationships from the commutation relation (A3). We have

$$aa^\dagger = a^\dagger a + 1 \ , \qquad aa^{\dagger 2} = (a^\dagger a + 1)a^\dagger = a^{\dagger 2} a + 2a^\dagger \ ,$$

and in general

$$aa^{\dagger n} = a^{\dagger n} a + n a^{\dagger n-1} \ . \tag{A5}$$

Let $|0\rangle$ denote the normalized state that satisfies the equation $a|0\rangle = 0$; and let $|n\rangle$ indicate the normalized state

$$|n\rangle = \frac{1}{\sqrt{n!}} a^{\dagger n}|0\rangle \ . \tag{A6}$$

The correctness of the normalization follows from the observation that

$$\langle 0|a^n a^{\dagger n}|0\rangle = \langle 0|a^{n-1} a a^{\dagger n}|0\rangle = n\,\langle 0|a^{n-1} a^{\dagger n-1}|0\rangle = n! \ ,$$

where use has been done of Eq. (A5). With similar procedures, we have that

$$a^\dagger a|n\rangle = n|n\rangle \ .$$

The number operator $a^\dagger a$ indicates the number of quanta (phonons) in the state $|n\rangle$. The eigenvalues of the Hamiltonian (A4) are thus $E_n = (n + \frac{1}{2})\hbar\omega$ with $n = 0, 1, 2 \ldots$.

From the expression (*A*6) of the normalized eigenstates of the harmonic oscillator, we see that the operators a and $a^\dagger$ satisfy the relations

$$a\,|n\rangle = \sqrt{n}\,|n-1\rangle \qquad a^\dagger\,|n\rangle = \sqrt{n+1}\,|n+1\rangle\ .$$

We also notice that

$$\langle n|a^{\dagger p}a^p|n\rangle = \langle n|a^{\dagger p}|n-p\rangle\langle n-p|a^p|n\rangle = (\sqrt{n-p+1}\cdot\ldots\cdot\sqrt{n})^2 \qquad n \geq p\ .$$

Thus

$$\langle n|a^{\dagger p}a^p|n\rangle = \begin{cases} n!/(n-p)! & \text{if } n \geq p \\ 0 & \text{if } n < p \end{cases}\ . \tag{A7}$$

Statistical average of operators

At thermodynamic equilibrium, the statistical average of an operator A is defined as

$$\langle A\rangle = \sum_{n=0}^{\infty} P_n \langle n|A|n\rangle\ , \tag{A8}$$

where

$$P_n = \frac{e^{-(n+\frac{1}{2})\hbar\omega/k_BT}}{\sum_m e^{-(m+\frac{1}{2})\hbar\omega/k_BT}} = \frac{e^{-n\hbar\omega/k_BT}}{\sum_m \left(e^{-\hbar\omega/k_BT}\right)^m}\ .$$

Summing up the geometric series in the denominator, and replacing into Eq. (*A*8), we have

$$\boxed{\langle A\rangle = (1-z)\sum_{n=0}^{\infty} z^n \langle n|A|n\rangle \quad \text{with} \quad z = \exp(-\hbar\omega/k_BT)}\ . \tag{A9}$$

Using Eq. (*A*9) we can obtain the thermal average of operators of interest. For instance, for the thermal average of the number operator we have

$$\langle a^\dagger a\rangle = (1-z)\sum_{n=0}^{\infty} z^n \langle n|a^\dagger a|n\rangle = (1-z)\sum_{n=0}^{\infty} n\, z^n$$

$$= (1-z)z\frac{\partial}{\partial z}\sum_{n=0}^{\infty} z^n = \frac{z}{1-z} = \frac{1}{e^{\hbar\omega/k_BT}-1}\ , \tag{A10}$$

which expresses the standard Bose–Einstein statistics. We also have

$$\langle a\,a^\dagger\rangle = \langle a^\dagger a\rangle + 1$$

$$\langle a\,a\rangle = \langle a^\dagger a^\dagger\rangle = 0\ .$$

With a little of algebra, we can prove the following relation

$$\boxed{\langle a^{\dagger p}a^p\rangle = p!\,\langle a^\dagger a\rangle^p} \tag{A11}$$

for any $p = 0, 1, 2, \ldots$. In fact, from Eq. $(A9)$ and Eq. $(A7)$ we have

$$\langle a^{\dagger p} a^p \rangle = (1-z) \sum_{n(\geq p)} \frac{n!}{(n-p)!} z^n = (1-z) \sum_{n=0}^{\infty} \frac{(n+p)!}{n!} z^{n+p} . \qquad (A12)$$

From Eq. $(A10)$ it follows

$$\langle a^\dagger a \rangle^p = \frac{z^p}{(1-z)^p} = \frac{(1-z)\, z^p}{(1-z)^{p+1}}$$

$$= (1-z)\, z^p \left[1 + (p+1)z + \frac{(p+1)(p+2)}{2!} z^2 + \ldots \right] = (1-z)\, z^p \sum_{n=0}^{\infty} \frac{(n+p)!}{n!\, p!} z^n . \qquad (A13)$$

From comparison of Eq. $(A12)$ and Eq. $(A13)$, we obtain Eq. $(A11)$.

Weyl identity

We establish now two identities (the Weyl identity and the Bloch identity), which are very useful in the study of the correlation functions and Debye–Waller factor in the scattering theory of the harmonic crystal (see Chapter X). We remember the Weyl identity, discussed in standard quantum mechanics textbooks [see for instance A. S. Davydov "Quantum Mechanics" (Pergamon Press, Oxford 1965) p.132].

Consider any two operators A and B, that commute with their commutator $[A, B]$; then we have

$$\boxed{e^A e^B = e^{A+B} e^{[A,B]/2}} \quad \text{if} \quad [A, [A, B]] \equiv [B, [A, B]] \equiv 0 . \qquad (A14)$$

The proof of the above identity can be performed, for instance, following a procedure due to Glauber. We replace momentarily the operators A and B by xA and xB, respectively, where the parameter x will be set equal to 1 at the end of the reasoning. We consider then the following two operators depending from the parameter x:

$$F_1(x) = e^{xA} e^{xB} \quad \text{and} \quad F_2(x) = e^{x(A+B)} e^{x^2 [A,B]/2} . \qquad (A15)$$

We show below that both functions $F_1(x)$ and $F_2(x)$ satisfy the differential equation

$$\frac{dF}{dx} = (A + B + x[A, B]) F(x) . \qquad (A16)$$

Eq. $(A16)$, together with the boundary condition $F_1(0) = F_2(0)$, implies $F_1(x) = F_2(x)$ for any x; in particular for $x = 1$ we have Eq. $(A14)$.

It is immediately seen that the function $F_2(x)$ satisfies Eq. $(A16)$; thus, we have only to prove that also $F_1(x)$ satisfies it. In fact

$$\frac{dF_1}{dx} = A\, e^{xA} e^{xB} + e^{xA}\, B\, e^{xB} = \left[A + e^{xA}\, B\, e^{-xA} \right] F_1(x) . \qquad (A17)$$

We now use the operatorial identity

$$e^{-S}\, O\, e^S = \left[1 - S + \frac{1}{2!} S^2 - \frac{1}{3!} S^3 + \ldots \right] O \left[1 + S + \frac{1}{2!} S^2 + \frac{1}{3!} S^3 + \ldots \right]$$

$$= O + [O,S] + \frac{1}{2!}[[O,S],S] + \frac{1}{3!}[[[O,S],S],S] + \dots \,, \qquad (A18)$$

which holds for any operator O and S. The particular case $S = -x\,A$ and $O = B$ gives $\exp(x\,A)\,B\,\exp(-x\,A) = B + x[A,B]$; this result, together with Eq. $(A17)$, proves that $F_1(x)$ satisfies the differential equation $(A16)$.

Bloch identity

We now prove that any operator C, arbitrary linear combination of phonon operators a and $a^\dagger$, satisfies the Bloch identity

$$\boxed{\langle e^C \rangle = e^{\langle C^2 \rangle/2}} \,; \qquad (A19)$$

this theorem states that the thermal average of the exponential of an operator, linear in a and $a^\dagger$, is just the exponential of half of the thermal average of the squared operator itself.

Consider in fact the linear combination of the phonon operators a and $a^\dagger$ of the form

$$C = c_1 a^\dagger + c_2 a$$

with c_1 and c_2 arbitrary complex numbers. We remark that

$$\langle C^2 \rangle = c_1 c_2 \left[2\langle a^\dagger a \rangle + 1 \right] \,.$$

Using the Weyl identity it follows

$$e^C = e^{c_1 a^\dagger + c_2 a} = e^{c_1 a^\dagger} e^{c_2 a} e^{c_1 c_2/2} \,.$$

Performing the thermal average one gets

$$\langle e^C \rangle = e^{c_1 c_2/2} \langle e^{c_1 a^\dagger} e^{c_2 a} \rangle = e^{c_1 c_2/2} \sum_{mn} \frac{c_1^m c_2^n}{m!\,n!} \langle a^{\dagger m} a^n \rangle \,.$$

In the double sum only the terms with $m = n$ survive, and using Eq. $(A11)$ it follows

$$\langle e^C \rangle = e^{c_1 c_2/2} \sum_m \frac{(c_1 c_2)^m}{m!} \langle a^\dagger a \rangle^m = e^{c_1 c_2 [2\langle a^\dagger a \rangle + 1]/2} \,,$$

and the Bloch identity is thus proved.

From the Bloch identity and the Weyl identity, we can obtain the following important result. Let A and B indicate two operators linear in creation and annihilation operators; it holds

$$\boxed{\langle e^A e^B \rangle = \langle e^{A+B} \rangle e^{[A,B]/2} = e^{\langle A^2 + 2AB + B^2 \rangle/2}} \,. \qquad (A20)$$

This relation will be used in Chapter X, in the study of the dynamical structure factor for the scattering of particles from harmonic crystals.

Further reading

H. Bilz and W. Kress "Phonon Dispersion Relations in Insulators" (Springer Verlag, Berlin 1979)

M. Born and K. Huang "Dynamical Theory of Crystal Lattices" (Oxford University Press 1954)

L. Brillouin "Wave Propagation in Periodic Structures" (Dover, New York 1953)

P. F. Choquard "The Anharmonic Crystal" (Benjamin, New York 1967)

B. Di Bartolo and R. C. Powell "Phonons and Resonances in Solids" (Wiley, New York 1976)

M. Dominoni and N. Terzi "How to Play with Springs and Pulses in a Classical Harmonic Crystal" in "Advances in Non-Radiative Processes in Solids" edited by B. Di Bartolo (Plenum Press, New York 1991).

H. Frölich "Theory of Dielectrics" (Clarendon Press, Oxford 1958)

G. Grimvall "The Electron – Phonon Interaction in Metals" (North-Holland, Amsterdam 1981)

M. E. Lines and A. M. Glass "Principles and Applications of Ferroelectric and Related Materials" (Clarendon Press, Oxford 1977)

H. A. Lorentz "The Theory of Electrons" (Dover, New York 1952)

A. A. Maradudin, E. W. Montroll, G. H. Weiss and I. P. Ipatova "Theory of Lattice Dynamics in the Harmonic Approximation" (Academic Press, New York 1971)

G. P. Srivastava "The Physics of Phonons" (Adam Hilger, Bristol 1990)

J. M. Ziman "Electrons and Phonons" (Clarendon Press, Oxford 1960)